

Counterion Effects on Propylene Polymerization Using Two-State *ansa*-Metallocene ComplexesMuqtar Mohammed,<sup>†</sup> Marcio Nele,<sup>‡</sup> Abdulaziz Al-Humydi,<sup>§</sup> Shixuan Xin,<sup>†</sup> Russell A. Stapleton,<sup>§</sup> and Scott Collins<sup>\*,§</sup>

Contribution from the Department of Chemistry, University of Waterloo,  
Waterloo, Ontario Canada, N2L 3G1, Progamma de Engenharia Quimica da COPPE,  
Universidade Federal do Rio de Janeiro, Rio de Janeiro - RJ, Brazil, and  
Department of Polymer Science, University of Akron, Akron, Ohio 44325-3909

Received June 3, 2002; E-mail: collins@polymer.uakron.edu

**Abstract:** Propylene polymerization using unsymmetrical, *ansa*-metallocene complexes  $\text{Me}_2\text{Y}(\text{Ind})\text{CpMMe}_2$  ( $\text{Y} = \text{Si}, \text{C}, \text{M} = \text{Zr}, \text{Y} = \text{C}, \text{M} = \text{Hf}$ ) and the co-initiators methyl aluminoxane (PMAO),  $\text{B}(\text{C}_6\text{F}_5)_3$ , and  $[\text{Ph}_3\text{C}][\text{B}(\text{C}_6\text{F}_5)_4]$  was studied at a variety of propylene concentrations. Modeling of the polymer microstructure reveals that the catalysts derived from  $\text{Me}_2\text{Si}(\text{Ind})\text{CpZrMe}_2$  and each of these co-initiators function under conditions where chain inversion is much faster than propagation (Curtin–Hammett conditions). Surprisingly, the microstructure of the PP formed was essentially unaffected by the nature of the counterion, suggesting similar values for the fundamental parameters inherent to two-state catalysts. The tacticity of PP was sensitive to changes in  $[\text{C}_3\text{H}_6]$  in the case of catalysts derived from  $\text{Me}_2\text{C}(\text{Ind})\text{CpHfMe}_2$  and PMAO, or  $[\text{Ph}_3\text{C}][\text{B}(\text{C}_6\text{F}_5)_4]$ , but the average tacticity of the polymer produced at a given  $[\text{C}_3\text{H}_6]$  decreased in the order  $[\text{Ph}_3\text{C}][\text{B}(\text{C}_6\text{F}_5)_4] > \text{PMAO}$ . With  $\text{B}(\text{C}_6\text{F}_5)_3$ , the polymer formed was more stereoregular, and its microstructure was invariant to changes in monomer concentration. The PP pentad distributions in this case could be modeled by assuming that all three catalyst/cocatalyst combinations function with different values for the relative rates of insertion to inversion ( $\Delta$ ) but otherwise feature essentially invariant, intrinsic stereoselectivity for monomer insertion ( $\alpha, \beta$ ), while the relative reactivity/stability ( $g/K$ ) of the isomeric ion-pairs present seems to be only modestly affected, if at all. Similar conclusions can also be made about the published propylene polymerization behavior of the  $\text{C}_s$ -symmetric  $\text{Me}_2\text{C}(\text{Flu})\text{CpZrMe}_2$  complex with different counterions. For every counterion investigated, the principle difference appears to be the operating regime ( $\Delta$ ) rather than intrinsic differences in insertion stereoselectivity ( $\alpha$ ). Surprisingly, the ordering of the various counterions with respect to  $\Delta$  does not agree with commonly accepted ideas about their coordinating ability. In particular, catalysts when activated with  $\text{B}(\text{C}_6\text{F}_5)_3$  appear to function at low values of  $\Delta$  as compared to those featuring  $\text{B}(\text{C}_6\text{F}_5)_4$  (less coordinating) and  $\text{FAI}[(o\text{-C}_6\text{F}_5)\text{C}_6\text{F}_4]_3$  (more coordinating) or PMAO (more coordinating) counterions where the ordering in  $\Delta$  is  $\text{MeB}(\text{C}_6\text{F}_5)_3 < \text{B}(\text{C}_6\text{F}_5)_4 < \text{FAI}[(o\text{-C}_6\text{F}_5)\text{C}_6\text{F}_4]_3 \approx \text{PMAO}$ . Possible reasons for this behavior are discussed.

## Introduction

The study of counteranion effects in metallocenium ion-catalyzed, olefin polymerization has revealed profound influences of the counteranion on catalyst stability, activity, and polymer molecular weight.<sup>1</sup> Such effects have been properly attributed to the degree of association of the counteranion with the metallocenium ion, including specific bonding interactions within contact ion-pairs in solution or the solid state, as well as the dynamics of these ion-pairs in solution.

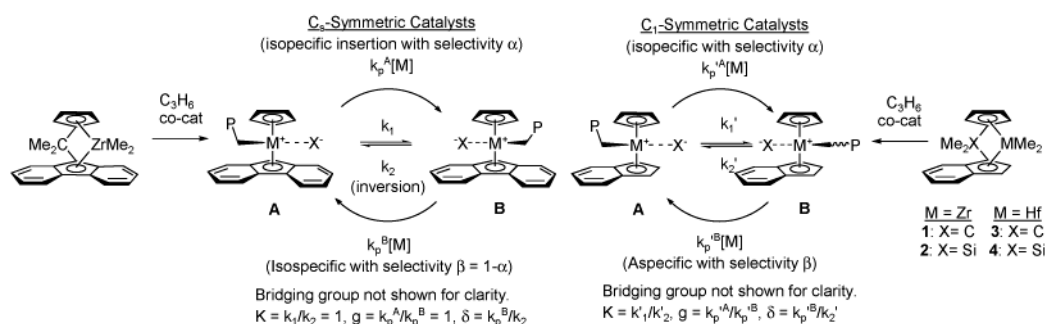
Surprisingly, the role(s) of the counteranion in influencing other features of olefin polymerization using metallocenium ions such as comonomer incorporation and/or poly(propylene) (PP) tacticity are less well understood.<sup>1</sup> While there was some early

evidence<sup>2</sup> that suggested counterion effects did not influence PP tacticity using  $\text{C}_2$ -symmetric metallocene catalysts, it would appear that strongly coordinating counteranions (e.g.,  $\text{FAI}[(o\text{-C}_6\text{F}_5)\text{C}_6\text{F}_4]_3$ ) markedly influence both the polymerization rate (large decrease) and the tacticity (significant increase) under controlled conditions.<sup>1,3</sup>

With  $\text{C}_s$ -symmetric complexes which produce s-PP, it would appear that strongly coordinating counteranions can increase polymer syndiotacticity again, at the expense of catalyst activity,<sup>3–4</sup> although here too there seems to be somewhat inconsistent data on this point in the literature.<sup>5</sup> Interestingly, solvent effects<sup>6</sup> can be important with this class of catalysts; a

<sup>†</sup> University of Waterloo.<sup>‡</sup> Universidade Federal do Rio de Janeiro.<sup>§</sup> University of Akron.(1) For a review, see: Chen, X.-Y.; Marks, T. J. *Chem. Rev.* **2000**, *100*, 1391–1434 and references therein.(2) (a) Chien, J. C. W.; Song, W.; Rausch, M. D. *Macromolecules* **1993**, *26*, 3239–3240. (b) Chien, J. C. W.; Rausch, M. D. *J. Polym. Sci., Part A: Polym. Chem.* **1994**, *32*, 2387–2393.(3) Chen, X.-Y.; Metz, M. V.; Li, L.; Stern, C. L.; Marks, T. J. *J. Am. Chem. Soc.* **1998**, *120*, 6287–6305.(4) (a) Chen, M.-C.; Marks, T. J. *Abstr. Pap. 221st ACS National Mtg.* **2001**, San Diego, CA, Inorganic Division, Paper 65. (b) Chen, M.-C.; Marks, T. J. *J. Am. Chem. Soc.* **2001**, *123*, 11803–11804.

Scheme 1



more polar solvent led to an increase in catalyst activity but a decrease in syndiotacticity.<sup>6b</sup> Recent work has clarified this issue in terms of a “leveling” effect on the relative rates of insertion versus chain back-skip, regardless of the counterion.<sup>4</sup>

Last, although counteranion effects on PP microstructure have been observed with  $C_1$ -symmetric complexes,<sup>7</sup> differing experimental conditions (e.g.,  $T$  and  $[C_3H_6]$ ) were involved which also can affect PP microstructure with catalysts of this type.<sup>8</sup>

We have recently described a kinetic approach for modeling stereosequence distributions in PP produced using two-state, bridged, or fluxional metallocene catalysts.<sup>9</sup> In favorable cases, analysis of the pentad distribution and its response to changes in  $[C_3H_6]$  at constant  $T$  for both  $C_1$ - and  $C_s$ -symmetric *ansa*-metallocene complexes can provide information on the intrinsic stereoselectivity of monomer insertion ( $\alpha$  and  $\beta$ , Scheme 1), the mechanism of stereocontrol at each of the two states (e.g., site vs chain-end control), as well as estimates for the relative reactivity/stability of two states (denoted by  $g/K$ , Scheme 1) and the ratio of the rate constants for monomer insertion with respect to chain back-skip or inversion for one of the states (denoted by  $\delta$ , Scheme 1).

It had occurred to us that counteranion effects might manifest themselves through changes to all of these fundamental quantities under a given set of conditions, resulting in PP with different microstructures and thus physical properties, simply by changing the counterion. On the basis of existing work,<sup>1–7</sup> it might be anticipated that, for example, significant changes to intrinsic stereoselectivity of the two states might only be accomplished through use of strongly coordinating counteranions – yet it was unclear how the other attributes of these types of catalyst

systems would be affected ( $g/K$  and  $\delta$ ) and how large an effect would be shown in, for example, the pentad distribution or other observable.

In this paper, we summarize the main features of our kinetic model, report the results of some propylene polymerization studies involving some simple unsymmetrical metallocene catalysts (1–4, Scheme 1) using different activators, and model the stereosequence distributions and their response to changes in polymerization conditions. In addition, we model some published data<sup>4b</sup> relating to the  $C_s$ -symmetric *ansa*-metallocene complex  $Me_2C(Cp)FluZrMe_2$  and different counterions. We believe the conclusions made about the effect of counterions on PP microstructure could prove to be general for this class of catalyst.

## Results and Discussion

**Summary of the Model.** Although we and others have written extensively about the basic features inherent to two-state polymerization catalysts<sup>8</sup> and how one can use a kinetic model to describe stereosequence distributions,<sup>9</sup> it is appropriate to review some of this material here.

In the case where the two states are enantiomeric (Scheme 1, left-hand side),  $g = K = 1$  by symmetry, while  $\beta = 1 - \alpha$ , and thus the polymerization behavior of  $C_s$ -symmetrical catalysts can be described by two fundamental parameters,  $\alpha$  and  $\delta$ . Both of these can be reliably estimated by studying the response of the pentad distribution to changes in  $[C_3H_6]$  at constant  $T$ , while the temperature-dependent behavior of  $\delta$  and  $\alpha$  can be elucidated by study of such catalysts at different  $T$  while varying  $[C_3H_6]$  at each  $T$ .<sup>9a</sup>

Note that we do not consider chain-end epimerization in the model. This is certainly expected at sufficiently low  $[M]$  with all *ansa*-metallocene complexes.<sup>10</sup> For the catalysts under study here, degradation in tacticity was not seen at the lowest  $[M]$  investigated, while it has been reported that the *rmmr* pentad does not uniformly increase with decreasing  $[M]$  (as would be expected for chain-end epimerization) with the  $Me_2C(Cp)$ - $FluZrMe_2$  catalyst activated by different cocatalysts.<sup>4</sup>

It is important to note that all  $C_s$ -symmetric (and indeed all) *ansa*-metallocene catalysts can be directly compared by defining a variable  $\Delta$  which represents the rate of insertion to inversion (i.e.,  $\Delta = \delta/[C_3H_6]$ , assuming first-order kinetics in monomer, Scheme 1). For example, if two  $C_s$ -symmetric catalysts produce polymer whose microstructure responds to changes in  $[C_3H_6]$  in an identical manner but one produces more stereoregular

- (5) Ewen, J. A. In *Catalyst Design for Tailor-Made Polyolefins*; Soga, K., Terano, M., Eds.; Elsevier: Tokyo, 1994; pp 405–410.
- (6) (a) Vizzini, J. C.; Chien, J. C. W.; Babu, G. N.; Newmark, R. A. *J. Polym. Sci., Part A: Polym. Chem.* **1994**, *32*, 2049–2056. (b) Herfert, N.; Fink, G. *Makromol. Chem.* **1992**, *193*, 773–8.
- (7) Giardello, M. A.; Eisen, M. S.; Stern, C. L.; Marks, T. J. *J. Am. Chem. Soc.* **1995**, *117*, 12114–12129 and references therein.
- (8) (a) Miller, S. A.; Bercaw, J. E. *Organometallics* **2002**, *21*, 934–945. (b) Veghini, D.; Henling, L. M.; Burkhardt, T. J.; Bercaw, J. E. *J. Am. Chem. Soc.* **1999**, *121*, 564–573. (c) Mohammed, M.; Xin, S.; Collins, S. *Am. Chem. Soc. PMSE Prepr.* **1999**, *80*, 441–442. (d) Kleinschmidt, R.; Refik, M.; Fink, G. *Macromol. Rapid Commun.* **1999**, *20*, 284–288. (e) Dietrich, U.; Hackmann, M.; Rieger, B.; Klinga, M.; Leskela, M. *J. Am. Chem. Soc.* **1999**, *121*, 4348–4355. (f) Bravakis, A. M.; Bailey, M. P.; Pigeon, M.; Collins, S. *Macromolecules* **1998**, *31*, 1000–1009. (g) Herzog, T. A.; Zubris, D. L.; Bercaw, J. E. *J. Am. Chem. Soc.* **1996**, *118*, 11988–11989. (h) Gauthier, W. J.; Corrigan, J. F.; Taylor, N. J.; Collins, S. *Macromolecules* **1995**, *28*, 3771–3778. (i) Gauthier, W. J.; Collins, S. *Macromolecules* **1995**, *28*, 3779–3786. (j) Rieger, B.; Jany, C.; Fawzi, R.; Steimann, M. *Organometallics* **1994**, *13*, 647–653.
- (9) (a) Nele, M.; Mohammed, M.; Xin, S.; Collins, S.; Pinto, J. C.; Dias, M. *Macromolecules* **2001**, *34*, 3830–3841. (b) Nele, M.; Collins, S.; Pinto, J. C.; Dias, M.; Lin, S.; Waymouth, R. M. *Macromolecules* **2000**, *33*, 7249–7260.

- (10) (a) Busico, V.; Caporaso, L.; Cipullo, R.; Landriani, L.; Angelini, G.; Margonelli, A.; Segre, A. L. *J. Am. Chem. Soc.* **1996**, *118*, 2105–2106. (b) Busico, V.; Cipullo, R. *J. Am. Chem. Soc.* **1994**, *116*, 9329–30.

polymer than the other, one may safely conclude that  $\alpha$  differs significantly between the two. If the two catalysts have identical values of  $\alpha$  but differ in their response to changes in  $[\text{C}_3\text{H}_6]$ , the pentad distributions that result will all fall on a single family of curves when plotted versus  $\Delta$ , and thus the differential effects on  $\delta$  for the two catalysts can be elucidated from their individual responses.

$C_1$ -symmetrical catalysts are more complicated in that  $g \neq K \neq 1$  and  $\beta \neq 1 - \alpha$  as the two states are diastereomeric (Scheme 1, right-hand side). A wider range of behavior is expected and observed depending on the magnitudes of the various parameters, while  $g/K$ ,  $\alpha$ ,  $\beta$ , and  $\delta$  can only be reliably estimated for catalysts functioning under conditions where  $\Delta \approx 1$ .

For either type of catalyst, one can define two extremes of behavior based on the magnitude of  $\Delta$ . If  $\Delta \ll 1$  under all conditions investigated, the two-state catalyst behaves like a single-state catalyst as the two states are fully equilibrated by the inversion process. During steady-state chain growth under these Curtin–Hammett (C–H) conditions, it can be shown that the average stereoselectivity of a given insertion is given by the following expression:  $\bar{\epsilon} = (\alpha(g/K) + \beta)/(g/K + 1)$ ,<sup>8f,9</sup> where  $\alpha$ ,  $\beta$ , and  $g/K$  are as defined in Scheme 1.

For a  $C_s$ -symmetric catalyst,  $\bar{\epsilon} = 0.5$ , and thus atactic PP will be produced, while for a  $C_1$ -symmetric catalyst, isotactic or atactic PP (or intermediate forms) may be formed depending on the magnitude of  $\alpha$ ,  $\beta$ , and  $g/K$ . In the usual situation with one state isospecific and the other stereorandom ( $\alpha \approx 1$ , while  $\beta \approx 0.5$ ), if  $g/K \gg 1$ , isotactic polymer will be produced.

When  $\Delta \gg 1$ , the two states are trapped by the insertion process – hence the term kinetic quenching (KQ); one forms polymer by an alternating insertion mechanism, and syndiotactic PP will be produced if both states are isospecific but with equal and opposite facial selectivity. Again, with  $C_1$ -symmetrical catalysts, one may form hemi-isotactic PP if  $\alpha \approx 1$  and  $\beta \approx 0.5$ , but other behavior is also observed.<sup>8a</sup>

Under C–H and KQ conditions, although PP microstructure will be largely invariant to changes in  $[\text{C}_3\text{H}_6]$ , one can distinguish between these two possibilities (except when  $\alpha = \beta$ ) as the stereosequence distributions are Bernoullian under the former conditions (single-state behavior). To go from one regime to another requires varying  $\Delta$  (i.e., monomer concentration) by about  $10^3$ , an impractical requirement. Thus, only catalysts which function under intermediate conditions ( $0.1 < \Delta < 10$ ) yield reliable estimates of all intrinsic parameters (2 for  $C_s$ - and 4 for  $C_1$ -symmetric catalysts). Further, as some of these parameters may be correlated with one another (e.g.,  $\alpha$  and  $g/K$  are frequently correlated as is evident in the equation for  $\bar{\epsilon}$ ),<sup>9a</sup> it is generally inappropriate to estimate these parameters on the basis of modeling the pentad (or higher  $n$ -ad) distribution obtained at a single  $[\text{C}_3\text{H}_6]$ .

In the case of  $C_s$ -symmetric catalysts, it is possible to estimate both  $\alpha$  and  $\delta$  using a pentad distribution obtained from a single experiment. However, we wish to emphasize that a complete pentad analysis using an appropriate model is important to extract meaningful estimates.

For example, the intensity of the “skipped defect”  $rmrr$  pentad in s-PP produced using  $\text{Me}_2\text{C}(\text{Cp})\text{FluZrX}_2$  catalyst is given by the following expression using our kinetic model, which is valid under all conditions, subject to the underlying assumptions of

first-order kinetics and the steady-state hypothesis being valid for intermediates involved in stereosequence formation:<sup>9</sup>

$$rmrr = \frac{\{2[\Delta^4(\alpha^2 - 2\alpha^3 + \alpha^4) + \Delta^3(4\alpha^4 - \alpha^3 - 3\alpha + 1) + \Delta^2(4\alpha^4 - 8\alpha^3 + 11\alpha^2 - 7\alpha + 3) + \Delta(4\alpha^2 - 4\alpha + 3) + 1]\}}{[(\Delta + 2)^4]} \quad (1)$$

There are higher order terms in  $\alpha$  and  $\Delta = \delta[\text{M}]$  including the product of the two, corresponding to the different ways of forming this pentad through a combination of skipped insertion and/or misinsertion. In the limit of  $\alpha = 1$ , eq 1 simplifies to

$$rmrr = \frac{2[\Delta^3 + 3\Delta^2 + 3\Delta + 1]}{(\Delta + 2)^4} = \frac{2(\Delta + 1)^3}{(\Delta + 2)^4} \quad (2)$$

and, in the limit  $\Delta \gg 2$ , this expression further simplifies to

$$rmrr = \frac{2}{\Delta} = \frac{2k_1}{k_p^A[\text{M}]} = \frac{2k_2}{k_p^B[\text{M}]} \quad (3)$$

In essence, only for  $C_s$ -symmetric catalysts functioning under KQ conditions and which are close to perfectly stereoregulating will the intensity of this pentad be directly equal to the ratio of the rates of inversion to insertion. One can easily show that, if  $rmrr = 0.08$  under the conditions investigated, this corresponds to  $\Delta = 19.6$  (assuming  $\alpha = 1$ ), whereas use of the simple equation  $rmrr = 2/\Delta$  gives  $\Delta = 25$ , an error of 28%. On the other hand, if  $rmrr = 0.02$ , the error in  $\Delta$  calculated using the approximate equation is only about 5%. Larger errors can be expected if  $\alpha$  is significantly less than 1.

We only point this out because one might be tempted to use the approximate relationship under all conditions, even where it is clearly invalid. A corollary to this is that if one is not sure what the magnitude of  $\Delta$  is at any particular  $[\text{M}]$ , estimation of both  $\alpha$  and  $\delta$  from the pentad distribution under these conditions will be less reliable than using estimates obtained from experiments at different  $[\text{M}]$ .

**Reaction of Dimethyl Complexes 1–4 with  $\text{B}(\text{C}_6\text{F}_5)_3$  and  $[\text{Ph}_3\text{C}][\text{B}(\text{C}_6\text{F}_5)_4]$ .** The simple, dimethylmetallocene complexes 1–4 (Scheme 1) were prepared as described in the literature<sup>11</sup> or in the Experimental Section. Detailed studies of the reaction of the Zr dimethyl complexes (1 and 2) with either  $\text{B}(\text{C}_6\text{F}_5)_3$  or  $[\text{Ph}_3\text{C}][\text{B}(\text{C}_6\text{F}_5)_4]$  in toluene or bromobenzene solution, respectively, have been conducted.<sup>12</sup> Some of the main observations to date will be summarized here to facilitate discussion.

In essence, isomeric ion-pairs are formed from 1 or 2 and  $\text{B}(\text{C}_6\text{F}_5)_3$  in toluene solution which are in slow exchange on the NMR time scale over the entire  $T$  range that they are stable ( $-80$  to ca.  $+50$  °C).<sup>13</sup> The major ion-pair present is 5 (Scheme 2) as shown by NOESY spectra (see Supporting Information), and the ratio of 5:6 varies from about 4:1 ( $\text{X} = \text{C}$ ) to 3:1 ( $\text{X} = \text{Si}$ ) and shows minor variation with  $T$  (increasing 5 at lower  $T$ ).

Insight into the nature of exchange processes involving these two isomeric ion-pairs was provided by EXSY spectroscopy.

- (11) (a) Compound 1: Cameron, P. A.; Gibson, V. C.; Graham, A. J. *Macromolecules* **2000**, *33*, 4329–4335. (b) Compounds 2–4: Mohammed, M. Ph.D. Thesis, University of Waterloo, 2001.
- (12) Mohammed, M.; Xin, S.; Al-Humydy, A.; Collins, S.; Monwar, M.; Rinaldi, P. L., manuscript in preparation.
- (13) The ion-pairs formed from the Zr complexes 1 and 2 have been studied in detail; their Hf analogues show qualitatively similar behavior.

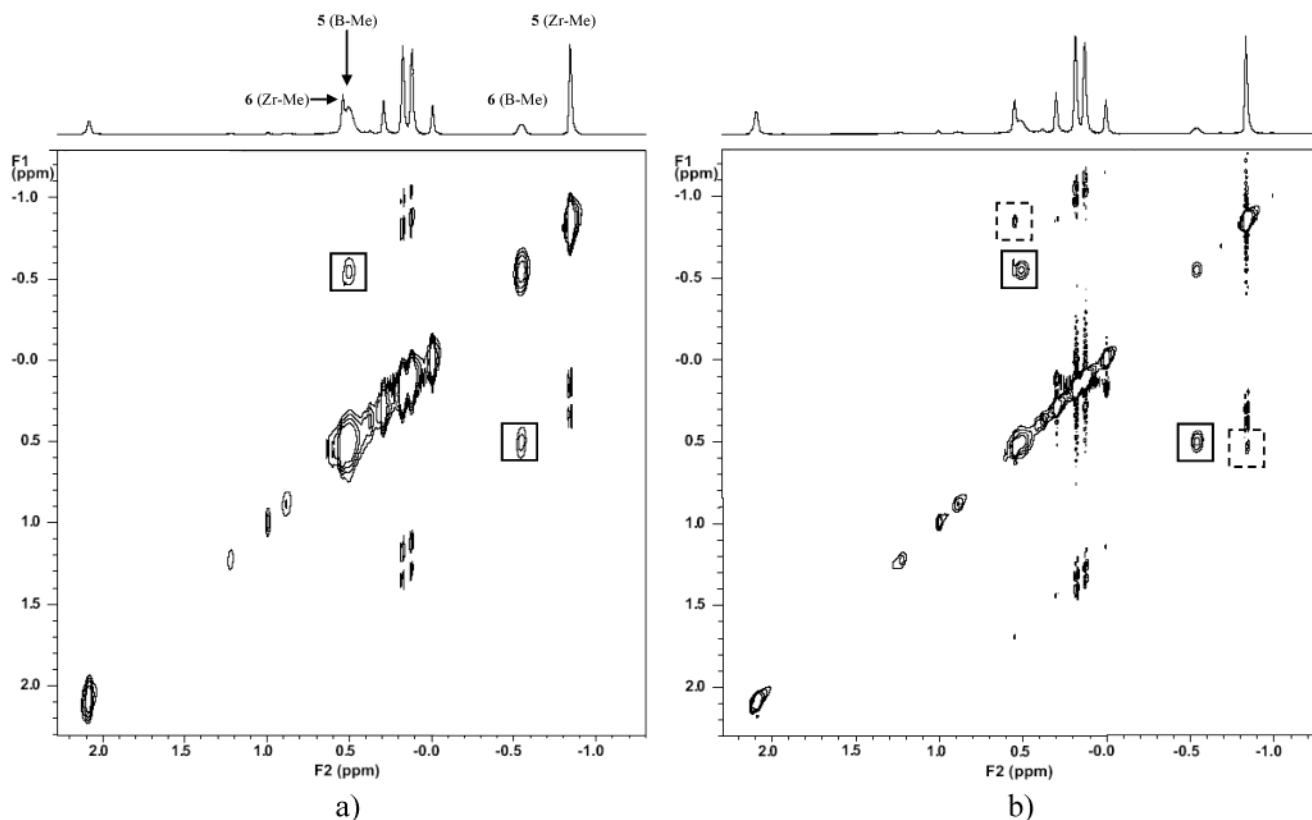
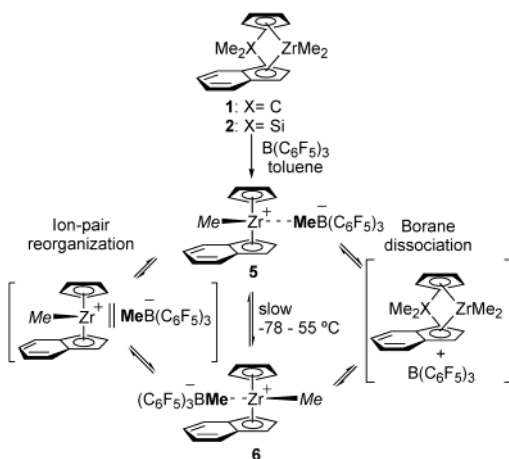


**Figure 1.** High field region ( $\delta$  -1.6 to 2.6) of the  $^1\text{H}$ - $^1\text{H}$  EXSY NMR spectra of ion-pairs **5** and **6** (X = Si) with peak assignments as shown. (a)  $\tau$  = 50 ms. (b)  $\tau$  = 500 ms. Exchange correlation peaks between B-Me and Zr-Me resonances are indicated with solid and dashed boxes, respectively.

#### Scheme 2



As shown in Figure 1, which depicts the high field region of the EXSY spectrum of ion-pairs **5** and **6** (X = Si), prominent exchange correlation between the B-Me signals of the two isomers is observed at short mixing times (50 ms, Figure 1a), while, in addition, weaker correlation is seen between the two Zr-Me signals at longer mixing times (500 ms, Figure 1b).

As indicated in Scheme 2, these two features are consistent with the overall process of ion-pair reorganization which permutes B-Me with B-Me and Zr-Me with Zr-Me signals on the different isomers rather than borane dissociation where B-Me signals are correlated with Zr-Me signals on different isomers.<sup>1</sup> However, because the B-Me signals exchange at very different rates than the Zr-Me signals, either the process of

ion-pair reorganization involves two distinct steps (Scheme 2) or a separate process leads to faster exchange of the B-Me signals.

Similar behavior has been observed elsewhere in a degenerate exchange process involving, for example, the ion-pair [*rac*-Me<sub>2</sub>-Si(2-Me-4'-Bu-Cp)<sub>2</sub>ZrMe][MeB(C<sub>6</sub>F<sub>5</sub>)<sub>3</sub>]<sup>14</sup> in benzene solution, where ion-pair reorganization leads to, for example, exchange correlation of the SiMe<sub>2</sub> signals. Rapid anion exchange between ion-pairs in a bimolecular fashion was invoked – that is, exchange of anions involving an ion-quadrupole as an intermediate. If this process were involved here, it would have to occur in a fashion where rapid exchange of anions occurs without change to the configuration of the metal in the two isomers; this seems somewhat unlikely but cannot be excluded on the basis of present evidence.

More recent work using [(1,2-Me<sub>2</sub>Cp)<sub>2</sub>ZrMe][MeB(C<sub>6</sub>F<sub>5</sub>)<sub>3</sub>] in bromobenzene at constant ionic strength and using [<sup>18</sup>Bu<sub>4</sub>N][MeB(C<sub>6</sub>F<sub>5</sub>)<sub>3</sub>] as a noninteracting source of the MeB(C<sub>6</sub>F<sub>5</sub>)<sub>3</sub> anion has revealed that ion-pair reorganization is a two-step process involving unimolecular, reversible, rate-determining dissociation of the anion followed by inversion at the metal.<sup>15</sup> We have seen similar behavior using ion-pairs **5** and **6** (X = C) in bromobenzene solution where again the B-Me signals exchange at a rate ( $k$  = 680 s<sup>-1</sup>) that is 34× faster than the overall rate of ion-pair reorganization ( $k'$  ≈ 20 s<sup>-1</sup> for the Zr-Me signals, see Supporting Information). This behavior is consistent with the mechanism proposed by Bercaw and Wendt

(14) Beck, S.; Lieber, S.; Schaper, F.; Geyer, A.; Brintzinger, H.-H. *J. Am. Chem. Soc.* **2001**, *123*, 1483–1489 and references therein.

(15) Wendt, O. F.; Bercaw, J. E., manuscript in preparation. Personal communication.



provided that the rate of (degenerate) anion reassociation is much faster than inversion from the intermediate, solvent-separated ion-pair in the case of **5** and **6**. Future work will focus on delineating these features.<sup>12</sup>

It should be mentioned that in the presence of excess borane (even trace quantities formed as a result of adventitious deactivation of the dialkyl used to form the ion-pairs) EXSY spectra reveal additional correlation between Zr–Me and B–Me resonances on different isomers which is more prominent at short mixing time than either of the two processes discussed above (see Supporting Information). As has been reported elsewhere,<sup>14</sup> the two isomeric ion-pairs may also interconvert by an independent mechanism which involves electrophilic attack of excess borane on the remaining Zr–Me group of these ion-pairs. Because, in the current case, this process is evidently more facile than either of the two unimolecular pathways (Scheme 2), it should be borne in mind in experiments of this kind. In particular, the exchange correlation peaks in the <sup>1</sup>H–<sup>1</sup>H EXSY spectra are identical to those expected for borane dissociation!

Analysis of the intensity data<sup>16</sup> from the EXSY spectrum shown in Figure 1b gives an estimate of the exchange rate constants of  $6 \pm 1$  and  $0.15 \pm 0.025 \text{ s}^{-1}$  for the two processes for the Si-bridged complex. In the case of the C-bridged analogue, the B–Me exchange process was detected at short mixing time and occurs at essentially the same rate ( $k_{\text{obs}} \approx 6 \pm 1 \text{ s}^{-1}$ ), while exchange correlation between the two Zr–Me signals was barely evident at the longest mixing time employed (5 s). An admittedly crude estimate of the overall rate of ion-pair reorganization of  $0.005 \pm 0.0025 \text{ s}^{-1}$  was obtained from the analysis of this EXSY spectrum. In comparing the Si- with C-bridged complex, it is therefore evident that ion-pair reorganization is about 30× faster in the former case at equivalent concentrations at 25 °C. This finding assumes prominence in view of the different polymerization behavior of these two catalysts (vide infra).

**Polymerization of Propylene Using Complexes 1–4 and Various Co-initiators.** Summarized in Table 1 are some polymerization rate and polymer property data for catalyst precursors **1–4** in combination with PMAO (1000–2000:1 Al:M), B(C<sub>6</sub>F<sub>5</sub>)<sub>3</sub> (1.2:1 B:M), or [Ph<sub>3</sub>C][B(C<sub>6</sub>F<sub>5</sub>)<sub>4</sub>] (1.2:1 B:M) at 30 °C and various [C<sub>3</sub>H<sub>6</sub>] in toluene solution. All combinations investigated gave rise to catalysts that were reasonably stable to the reaction conditions as revealed by stable mass flow profiles with time following attainment of steady-state conditions (see Figure 2, for example). As would be expected, polymerization activity ( $R_p$ ) tracks with the nature of the counterion with B(C<sub>6</sub>F<sub>5</sub>)<sub>4</sub> ≈ MeMAO > MeB(C<sub>6</sub>F<sub>5</sub>)<sub>3</sub>, while polymer MW varies to a lesser degree [B(C<sub>6</sub>F<sub>5</sub>)<sub>4</sub> > MeB(C<sub>6</sub>F<sub>5</sub>)<sub>3</sub> ≈ MeMAO] and with the usual dependencies on Zr versus Hf.

In the case of the boron-based co-initiators, an excess of MeAl(BHT)<sub>2</sub> (MAD) was used as an “noninteracting” scrubbing agent (ca. 0.5–2 mM MAD).<sup>17</sup> Earlier we reported that this compound does not react with B(C<sub>6</sub>F<sub>5</sub>)<sub>3</sub> or the metallocenium ion derived from reaction of this activator with, for example, Cp<sub>2</sub>ZrMe<sub>2</sub> or act as an inhibitor of catalyst activity even when present in large excess. Similar comments also apply to the ion-

**Table 1.** Polymerization of Propylene Using Complexes **1–4** and Various Cocatalysts<sup>a</sup>

entry	complex	cocat <sup>b</sup>	[M] (μM)	[C <sub>3</sub> H <sub>6</sub> ]	$R_p^c$	$M_w$ (K)	$M_w/M_n$	%mmm
1	<b>1</b>	A	20	1.30	10	1.73	2.7	12
2	<b>1</b>	A	20	2.21	17	1.92	2.7	14
3	<b>1</b>	A	20	3.26	26	2.01	3.0	12
4	<b>1</b>	B	5	1.76	27	2.24	2.3	12
5	<b>2</b>	A	2.5	1.15	25	11.6	1.7	31
6	<b>2</b>	A	2.5	2.21	68	13.3	1.8	31
7	<b>2</b>	A	2.5	3.26	104	14.9	1.8	34
8	<b>2</b>	B	10	1.76	49	19.0	2.4	34
9	<b>2</b>	B	10	2.48	79	26.9	1.7	34
10	<b>2</b>	B	10	3.26	91	26.2	1.8	34
11	<b>2</b>	C	15	1.76	11	16.3	1.8	34
12	<b>2</b>	C	15	2.48	15	15.3	2.1	35
13	<b>2</b>	C	15	3.26	20	16.2	2.2	35
14	<b>3</b>	A	20	0.96	1.5	26.2	2.3	38
15	<b>3</b>	A	20	2.21	3.4	38.9	1.9	30
16	<b>3</b>	A	20	4.18	5.5	48.1	2.0	28
17	<b>3</b>	A	20	8.82	<i>d</i>	43.2	2.0	23
18	<b>3</b>	B	5.0	0.96	12	32.3	1.8	44
19	<b>3</b>	B	5.0	1.76	43	39.6	1.8	44
20	<b>3</b>	B	5.0	3.26	64	39.4	1.6	39
21	<b>3</b>	B	2.5	4.41	81	42.2	1.7	38
22	<b>3</b>	C	20	1.30	2.0	22.2	2.1	48
23	<b>3</b>	C	15	1.76	2.8	35.3	1.9	47
24	<b>3</b>	C	20	2.21	3.8	34.2	1.7	47
25	<b>3</b>	C	20	3.26	6.9	38.2	1.7	48
26	<b>4</b>	A	20	1.15	7.5	99.1	2.2	51
27	<b>4</b>	A	20	2.21	14	152	2.0	52
28	<b>4</b>	A	20	3.26	19	188	2.8	52

<sup>a</sup> Conditions: toluene solution (300–500 mL), 30 °C, 1000 rpm, 30–120 min reaction time depending on catalyst/activator. <sup>b</sup> A = solid PMAO (1000:1 M = Zr; 2000:1 M = Hf); B = [Ph<sub>3</sub>C][B(C<sub>6</sub>F<sub>5</sub>)<sub>4</sub>] (1.2:1 B:M) added to reactor (presaturated with monomer and containing ca. 1–2 mM of MAD) 1–2 min prior to complex **1–4**; C = B(C<sub>6</sub>F<sub>5</sub>)<sub>3</sub> and metallocene complex (1.2:1 B:M) combined in 20 mL of toluene at 25 °C and then added to reactor presaturated with monomer and containing ca. 1–2 mM of MAD. <sup>c</sup> Steady-state  $R_p$  [mol C<sub>3</sub>H<sub>6</sub>/[M] × s)] as measured by calibrated mass flow meters (for representative flow profiles, see Figure 2). <sup>d</sup> Polymerization in liquid propylene, activity is  $1.1 \times 10^5 \text{ g of PP/mol Hf} \times \text{h}$ .

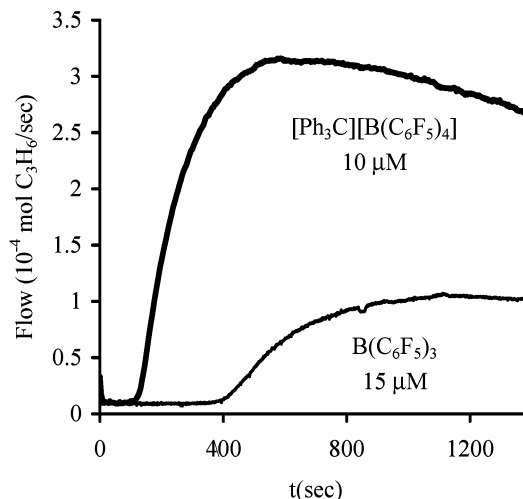


**Figure 2.** Propylene flow ( $10^{-4} \text{ mol C}_3\text{H}_6 \text{ s}^{-1}$ ) vs time (s) for catalyst **2** activated by B(C<sub>6</sub>F<sub>5</sub>)<sub>3</sub> and [Ph<sub>3</sub>C][B(C<sub>6</sub>F<sub>5</sub>)<sub>4</sub>]. The time period between catalyst injection and uptake of monomer corresponds to consumption of a fixed quantity ( $\sim 0.4 \text{ g}$  at 30 °C and 30 psi) of dissolved monomer so as to produce a measurable pressure drop leading to initiation of flow. A more active catalyst features a shorter lag time between injection and detection of flow.

(16) Observed rate constants were calculated from  $k_{\text{obs}} = (1/\tau_m) \ln[(r+1)/(r-1)]$ , where  $\tau_m$  is the mixing time, and  $r = \Sigma I_d / \Sigma I_x$ , where  $I_d$  and  $I_x$  are the intensities of the diagonal and cross-peaks, respectively. See: Perrin, C. L.; Dwyer, T. J. *Chem. Rev.* **1990**, *90*, 935.

pairs (**5** and **6**, X = Si, [Zr] = 0.025 M) under study here; both <sup>1</sup>H and <sup>19</sup>F NMR spectra were unchanged in the presence of ca. 5 equiv of this additive ([Al]  $\approx$  0.125 M) after 1 h at 25 °C

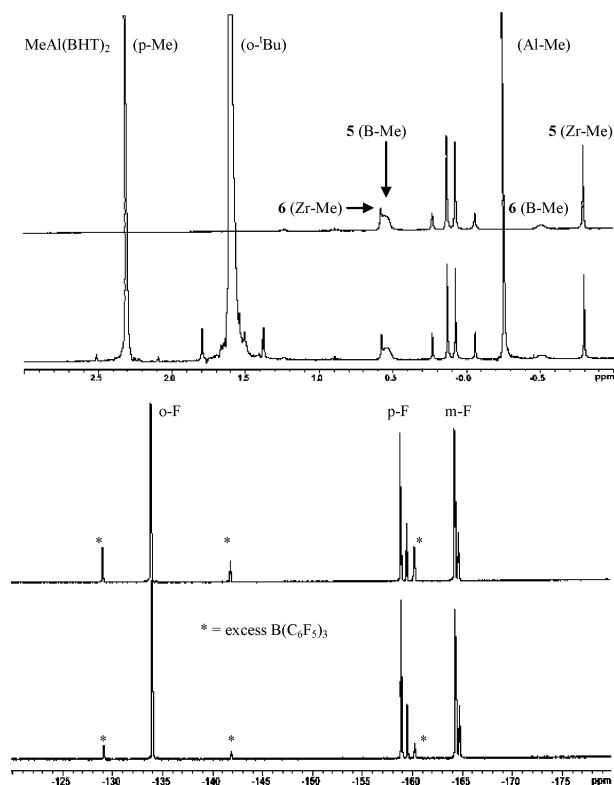


**Figure 3.**  $^1\text{H}$  and  $^{19}\text{F}$  NMR spectra of ion-pairs **5** and **6** ( $\text{X} = \text{Si}$ ) in the absence and presence of 5 equiv of  $\text{MeAl}(\text{BHT})_2$  after 1 h at 25 °C with  $[\text{Zr}] = 0.025 \text{ M}$  and  $[\text{Al}] \approx 0.125 \text{ M}$ .

as shown in Figure 3. Because the absolute concentrations of Zr and Al were  $>10^3$  and  $125\times$  greater in this experiment than those under polymerization conditions (i.e.,  $[\text{Zr}] = 2\text{--}20 \mu\text{M}$  and  $[\text{Al}] < 2 \text{ mM}$ ), we can conclude that, on the time scale of these polymerization experiments (i.e., 1–10 h) and at the concentrations employed,  $\text{MeAl}(\text{BHT})_2$  is inert toward these ion-pairs and does not modify their chemistry.

$\text{MeAl}(\text{BHT})_2$  is not inert toward  $[\text{Ph}_3\text{C}][\text{B}(\text{C}_6\text{F}_5)_4]$  and undergoes slow hydride abstraction to form  $\text{Ph}_3\text{CH}$  and unidentified Al byproducts in bromobenzene at room temperature ( $t_{1/2} \approx 1.5 \text{ h}$  at  $[\text{Ph}_3\text{C}][\text{B}(\text{C}_6\text{F}_5)_4] = [\text{MAD}] = 0.0086 \text{ M}$ ). For this reason, in polymerization reactions using this activator, the dimethylmetallocene was added separately, but immediately after adding  $[\text{Ph}_3\text{C}][\text{B}(\text{C}_6\text{F}_5)_4]$  to the reactor presaturated with monomer and containing excess MAD. We have previously shown that this procedure minimizes initial degradation of active cocatalyst in ethylene polymerization involving  $\text{Cp}_2\text{ZrMe}_2$  and this activator.<sup>17c</sup>

In comparing the behavior of the different activators employed, we noted that catalysts activated by  $\text{B}(\text{C}_6\text{F}_5)_3$  exhibited a slow buildup to steady-state conditions, corresponding to a constant concentration of growing chains, as compared to the  $[\text{Ph}_3\text{C}][\text{B}(\text{C}_6\text{F}_5)_4]$  activator. As indicated in Figure 2, attainment of steady-state conditions required nearly 40 min at 30 °C using preformed ion-pairs at  $[\text{Zr}] = 15 \mu\text{M}$ , while use of  $[\text{Ph}_3\text{C}]$ -

$[\text{B}(\text{C}_6\text{F}_5)_4]$  required about 15 min to reach steady-state, despite lower concentrations and in situ catalyst formation. The slower buildup to steady state is consistent with slow initiation relative to propagation in the case of the borane-activated complexes. This behavior has been previously observed and quantified in the polymerization of 1-hexene using  $[\text{en}(\text{Ind})_2\text{ZrMe}][\text{MeB}(\text{C}_6\text{F}_5)_3]$  where  $k_p/k_i \approx 70$ .<sup>18</sup>

It is worth pointing out that the values of  $R_p$  reported in Table 1 were those measured at steady-state following completion of initiation and are thus characteristic of intrinsic catalyst activity. As the results in the Figure 2 indicate, the difference in steady-state rates of monomer consumption is only about a factor of 5 for these two counterions with  $\text{B}(\text{C}_6\text{F}_5)_4 > \text{MeB}(\text{C}_6\text{F}_5)_3$ .

As far as PP microstructure is concerned, of the various complexes and co-initiators investigated, only the Hf complex **3** produced PP whose microstructure was sensitive to the nature of the counterion or to changes in  $[\text{C}_3\text{H}_6]$  ( $m\text{mmmm} = 23\text{--}48\%$ , Table 1, entries 14–25). Zirconium complexes **1** and **2** furnished oligomeric, “hemi-isotactic” PP ( $m\text{mmmm} \leq 15\%$ , entries 1–4) and higher MW, marginally isotactic PP ( $m\text{mmmm} \approx 32\text{--}35\%$ , entries 5–13), respectively, while the Hf analogue of **2** (**4**) furnished more stereoregular PP ( $m\text{mmmm} \approx 52\%$ , entries 26–28) whose microstructure was also invariant to changes in monomer concentration.

In the case of complex **1** activated by PMAO, where oligo-PP microstructure is insensitive to changes in  $[\text{C}_3\text{H}_6]$  (Table 1, entries 1–3), we were unable to precisely fit the pentad distributions to either limiting form (C–H or KQ) of our model, even after correction of the pentad distribution for interference from end groups.<sup>9</sup> We suspect this result simply reflects the inadequacy of our model (in particular, our model is only valid where the kinetic chain length  $= R_p/R_{tr} = \bar{X}_n$  is long compared to a pentad) rather than anything peculiar about this complex. In view of this inadequacy, we did not systematically investigate different activators, etc. with this catalyst particularly when use of  $[\text{Ph}_3\text{C}][\text{B}(\text{C}_6\text{F}_5)_4]$  as an activator led to no change in microstructure and insignificant changes in the degree of polymerization (entry 4 vs 1–3).

In the case of Si-bridged complexes **2** and **4** where again no significant variation in microstructure was found on varying  $[\text{C}_3\text{H}_6]$  (Table 1, entries 5–13 and 26–28), we had earlier shown that both of these complexes behave as single-state catalysts on activation with PMAO.<sup>9a</sup> We therefore felt it was instructive to only study the effect of counterion with one of these complexes (**2**) as limited information is available from analysis of the pentad distribution under C–H conditions (i.e., one parameter).

Selected pentad distributions and those calculated using our kinetic model are summarized in Table 2; complete results are provided as Supporting Information. As can be gleaned from the data in Table 2, the pentad distributions of PP formed using complex **2** (entries 6, 9, and 12) and the various activators are essentially the same, invariant to changes in  $[\text{C}_3\text{H}_6]$  and completely consistent with single-state behavior. As indicated in the Introduction, only a single parameter  $\bar{e}$  can be extracted through analysis of the (Bernoullian) pentad distributions under C–H conditions, and the fact that this parameter is the same for all three cocatalysts (Table 3) implies that the fundamental

(17) (a) Williams, V. C.; Dai, C.; Li, Z.; Collins, S.; Piers, W. E.; Clegg, W.; Elsegood, M. R. J.; Marder, T. B. *Angew. Chem., Int. Ed.* **1999**, *38*, 3695–3698. (b) Vollmerhaus, R.; Rahim, M.; Tomaszewski, R.; Xin, S.; Taylor, N. J.; Collins, S. *Organometallics* **2000**, *19*, 2161–2169. (c) Williams, V. C.; Irvine, G. J.; Piers, W. E.; Li, Z.; Collins, S.; Clegg, W.; Elsegood, M. R. J.; Marder, T. B. *Organometallics* **2000**, *19*, 1619–1621. (d) Metcalfe, R. A.; Kreller, D. I.; Tian, J.; Kim, H.; Taylor, N. J.; Corrigan, J. F.; Collins, S. *Organometallics* **2002**, *21*, 1719–1726.

(18) Liu, Z.; Somsook, E.; White, C. B.; Rosaaen, K. A.; Landis, C. R. *J. Am. Chem. Soc.* **2001**, *123*, 11193–11207.

**Table 2.** Selected Pentad Distributions of PP Prepared Using Two-State *ansa*-Metallocene Complexes<sup>a</sup>

Complexes 1–3 and Various Cocatalysts (this work)									
entry <sup>b</sup>	mmmm	mmmr	rmrr	mmrr	xmrx	mrmr	rrrr	rrrm	mrrm
2	0.13 <sub>7</sub> (0.13 <sub>7</sub> )	0.14 <sub>8</sub> (0.13 <sub>8</sub> )	0.05 <sub>3</sub> (0.05 <sub>5</sub> )	0.18 <sub>2</sub> (0.17 <sub>0</sub> )	0.15 <sub>2</sub> (0.15 <sub>8</sub> )	0.05 <sub>9</sub> (0.07 <sub>9</sub> )	0.06 <sub>9</sub> (0.08 <sub>3</sub> )	0.12 <sub>8</sub> (0.11 <sub>1</sub> )	0.10 <sub>8</sub> (0.06 <sub>9</sub> )
4	0.11 <sub>8</sub> (0.13 <sub>1</sub> )	0.13 <sub>8</sub> (0.13 <sub>8</sub> )	0.05 <sub>4</sub> (0.05 <sub>5</sub> )	0.16 <sub>3</sub> (0.16 <sub>5</sub> )	0.15 <sub>5</sub> (0.16 <sub>7</sub> )	0.07 <sub>5</sub> (0.08 <sub>4</sub> )	0.06 <sub>0</sub> (0.07 <sub>9</sub> )	0.14 <sub>1</sub> (0.11 <sub>1</sub> )	0.12 <sub>6</sub> (0.06 <sub>9</sub> )
6	0.31 <sub>4</sub> (0.33 <sub>2</sub> )	0.17 <sub>6</sub> (0.16 <sub>6</sub> )	0.04 <sub>5</sub> (0.02 <sub>5</sub> )	0.15 <sub>3</sub> (0.16 <sub>6</sub> )	0.10 <sub>4</sub> (0.10 <sub>1</sub> )	0.05 <sub>7</sub> (0.05 <sub>1</sub> )	0.02 <sub>5</sub> (0.02 <sub>5</sub> )	0.05 <sub>5</sub> (0.05 <sub>1</sub> )	0.08 <sub>5</sub> (0.08 <sub>3</sub> )
9	0.34 <sub>1</sub> (0.33 <sub>7</sub> )	0.19 <sub>4</sub> (0.16 <sub>6</sub> )	0.02 <sub>4</sub> (0.02 <sub>5</sub> )	0.17 <sub>1</sub> (0.16 <sub>6</sub> )	0.10 <sub>2</sub> (0.09 <sub>9</sub> )	0.05 <sub>4</sub> (0.05 <sub>0</sub> )	0.01 <sub>3</sub> (0.02 <sub>5</sub> )	0.03 <sub>2</sub> (0.05 <sub>0</sub> )	0.07 <sub>4</sub> (0.08 <sub>3</sub> )
12	0.34 <sub>6</sub> (0.34 <sub>2</sub> )	0.19 <sub>4</sub> (0.16 <sub>6</sub> )	0.02 <sub>4</sub> (0.02 <sub>4</sub> )	0.16 <sub>2</sub> (0.16 <sub>6</sub> )	0.10 <sub>4</sub> (0.09 <sub>7</sub> )	0.05 <sub>4</sub> (0.04 <sub>9</sub> )	0.01 <sub>3</sub> (0.02 <sub>4</sub> )	0.03 <sub>5</sub> (0.04 <sub>9</sub> )	0.07 <sub>5</sub> (0.08 <sub>3</sub> )
15	0.30 <sub>3</sub> (0.31 <sub>3</sub> )	0.17 <sub>3</sub> (0.16 <sub>6</sub> )	0.03 <sub>3</sub> (0.02 <sub>5</sub> )	0.19 <sub>5</sub> (0.18 <sub>9</sub> )	0.07 <sub>2</sub> (0.08 <sub>0</sub> )	0.02 <sub>7</sub> (0.03 <sub>1</sub> )	0.04 <sub>0</sub> (0.04 <sub>3</sub> )	0.07 <sub>2</sub> (0.06 <sub>5</sub> )	0.09 <sub>7</sub> (0.08 <sub>8</sub> )
19	0.44 <sub>3</sub> (0.43 <sub>1</sub> )	0.17 <sub>0</sub> (0.16 <sub>0</sub> )	0.02 <sub>2</sub> (0.01 <sub>7</sub> )	0.17 <sub>1</sub> (0.16 <sub>5</sub> )	0.05 <sub>1</sub> (0.06 <sub>3</sub> )	0.01 <sub>4</sub> (0.02 <sub>9</sub> )	0.01 <sub>9</sub> (0.01 <sub>9</sub> )	0.02 <sub>4</sub> (0.03 <sub>5</sub> )	0.08 <sub>8</sub> (0.08 <sub>2</sub> )
23	0.46 <sub>8</sub> (0.48 <sub>3</sub> )	0.16 <sub>7</sub> (0.15 <sub>2</sub> )	0.02 <sub>1</sub> (0.01 <sub>4</sub> )	0.16 <sub>5</sub> (0.15 <sub>3</sub> )	0.04 <sub>9</sub> (0.05 <sub>4</sub> )	0.01 <sub>4</sub> (0.02 <sub>7</sub> )	0.01 <sub>2</sub> (0.01 <sub>4</sub> )	0.02 <sub>4</sub> (0.02 <sub>8</sub> )	0.08 <sub>1</sub> (0.07 <sub>6</sub> )
Me <sub>2</sub> C(Cp)FluZrMe <sub>2</sub> and Various Cocatalysts (refs 4b and 9a) <sup>c</sup>									
cocat <sup>d</sup>	mmmm	mmmr	rmrr	mmrr	xmrx	mrmr	rrrr	rrrm	mrrm
A <sup>e</sup>			0.02 <sub>1</sub>	0.04 <sub>3</sub>	0.03 <sub>7</sub>		0.81 <sub>5</sub>		
B			0.02 <sub>0</sub>	0.04 <sub>4</sub>	0.10 <sub>7</sub>		0.64 <sub>9</sub>		
			0.02 <sub>2</sub>	0.04 <sub>6</sub>	0.11 <sub>6</sub>		0.64 <sub>5</sub>		
C			0.02 <sub>7</sub>	0.05 <sub>6</sub>	0.17 <sub>1</sub>		0.45 <sub>5</sub>		
			0.03 <sub>0</sub>	0.06 <sub>5</sub>	0.18 <sub>0</sub>		0.45 <sub>8</sub>		
D			0.02 <sub>1</sub>	0.04 <sub>0</sub>	0.04 <sub>9</sub>		0.79 <sub>1</sub>		
			0.02 <sub>1</sub>	0.04 <sub>4</sub>	0.04 <sub>9</sub>		0.79 <sub>0</sub>		

<sup>a</sup> Observed values with calculated values in parentheses – full details are included as Supporting Information. <sup>b</sup> Entries correspond to those in Table 1. <sup>c</sup> Conditions: toluene solution, 60 °C, 3 atm C<sub>3</sub>H<sub>6</sub>, 1000 rpm with [Zr] = 1–10 μM or see ref 4b. <sup>d</sup> A = PMAO (1000:1 Al:Zr); B = [Ph<sub>3</sub>C][B(C<sub>6</sub>F<sub>5</sub>)<sub>4</sub>]; C = B(C<sub>6</sub>F<sub>5</sub>)<sub>3</sub>; D = [Ph<sub>3</sub>C][FAI(*o*-C<sub>6</sub>F<sub>5</sub>-C<sub>6</sub>F<sub>4</sub>)<sub>3</sub>]. <sup>e</sup> Calculated values extrapolated from data obtained at 30–50 °C using the known *T* dependence of  $\delta$  – see ref 9a.

**Table 3.** Modeling of PP Microstructure Produced Using Two-State *ansa*-Metallocene Complexes<sup>a</sup>

cocatalyst	$\alpha$	$\beta$	<i>g/K</i>	$\delta$	( $\sigma^2$ ) <sup>b</sup>
Me <sub>2</sub> Si(Cp)IndZrMe <sub>2</sub> (2)					
PMAO	$\bar{\epsilon}$ = 0.802		<i>c</i>	5.9 × 10 <sup>−4</sup>	
[Ph <sub>3</sub> C][B(C <sub>6</sub> F <sub>5</sub> ) <sub>4</sub> ]	$\bar{\epsilon}$ = 0.804		<i>c</i>	1.5 × 10 <sup>−3</sup>	
B(C <sub>6</sub> F <sub>5</sub> ) <sub>3</sub>	$\bar{\epsilon}$ = 0.807		<i>c</i>	1.6 × 10 <sup>−3</sup>	
Me <sub>2</sub> C(Cp)IndHfMe <sub>2</sub> (3) (Scenario I – $\alpha$ , $\beta$ , and <i>g/K</i> the same)					
PMAO	0.95 <sub>3</sub>	0.57 <sub>8</sub>	3.4 <sub>8</sub>	0.52 <sub>4</sub>	1.1 × 10 <sup>−3</sup>
[Ph <sub>3</sub> C][B(C <sub>6</sub> F <sub>5</sub> ) <sub>4</sub> ]	0.95 <sub>3</sub>	0.57 <sub>8</sub>	3.4 <sub>8</sub>	0.094 <sub>2</sub>	7.3 × 10 <sup>−4</sup>
B(C <sub>6</sub> F <sub>5</sub> ) <sub>3</sub>	0.95 <sub>3</sub>	0.57 <sub>8</sub>	3.4 <sub>8</sub>	0.021 <sub>8</sub>	2.0 × 10 <sup>−3</sup>
Complex 3 (Scenario II – $\alpha$ and $\beta$ the same, <i>g/K</i> different)					
PMAO	0.92	0.61	14	0.82 <sub>4</sub>	1.0 × 10 <sup>−3</sup>
[Ph <sub>3</sub> C][B(C <sub>6</sub> F <sub>5</sub> ) <sub>4</sub> ]	0.92	0.61	5.3	0.095 <sub>3</sub>	7.4 × 10 <sup>−4</sup>
B(C <sub>6</sub> F <sub>5</sub> ) <sub>3</sub>	0.92	0.61	4.8	0.011 <sub>7</sub>	2.0 × 10 <sup>−3</sup>
Me <sub>2</sub> C(Cp)FluZrMe <sub>2</sub> (Scenario I – same $\alpha$ )					
PMAO	0.97 <sub>4</sub>	0.02 <sub>6</sub> <sup>d</sup>	1	39.4	<i>e</i>
[Ph <sub>3</sub> C][FAI( <i>o</i> -C <sub>6</sub> F <sub>5</sub> -C <sub>6</sub> F <sub>4</sub> ) <sub>3</sub> ]	0.97 <sub>4</sub>	0.02 <sub>6</sub>	1	31.8	1.0 × 10 <sup>−4</sup>
[Ph <sub>3</sub> C][B(C <sub>6</sub> F <sub>5</sub> ) <sub>4</sub> ]	0.97 <sub>4</sub>	0.02 <sub>6</sub>	1	9.9 <sub>9</sub>	3.4 × 10 <sup>−4</sup>
B(C <sub>6</sub> F <sub>5</sub> ) <sub>3</sub>	0.97 <sub>4</sub>	0.02 <sub>6</sub>	1	4.0 <sub>2</sub>	4.5 × 10 <sup>−4</sup>
Me <sub>2</sub> C(Cp)FluZrMe <sub>2</sub> (Scenario II – different $\alpha$ )					
PMAO <sup>b</sup>	0.97 <sub>5</sub>	0.02 <sub>5</sub> <sup>d</sup>	1	39.4	<i>e</i>
[Ph <sub>3</sub> C][FAI( <i>o</i> -C <sub>6</sub> F <sub>5</sub> -C <sub>6</sub> F <sub>4</sub> ) <sub>3</sub> ]	0.97 <sub>5</sub>	0.02 <sub>5</sub>	1	31.1	1.0 × 10 <sup>−4</sup>
[Ph <sub>3</sub> C][B(C <sub>6</sub> F <sub>5</sub> ) <sub>4</sub> ]	0.97 <sub>5</sub>	0.02 <sub>5</sub>	1	9.7 <sub>8</sub>	3.3 × 10 <sup>−4</sup>
B(C <sub>6</sub> F <sub>5</sub> ) <sub>3</sub>	0.96 <sub>6</sub>	0.03 <sub>4</sub>	1	4.3 <sub>3</sub>	3.4 × 10 <sup>−4</sup>

<sup>a</sup> For definition of parameters and model description, see introduction and ref 9a. <sup>b</sup> Standard variance of the fit, normalized to the number of experiments. <sup>c</sup> Curtin–Hammett conditions apply (Bernoullian distribution), and  $\delta$  cannot be unambiguously determined. <sup>d</sup>  $\beta$  is equal to 1 –  $\alpha$ . <sup>e</sup> The data used for modeling purposes were extrapolated from earlier work at 30–50 °C – an error estimate is not applicable.

parameters  $\alpha$ ,  $\beta$ , and *g/K* are also similar for the different counterions investigated.

Also, despite significant differences in *R<sub>p</sub>* for the different activators investigated, spanning about an order of magnitude

at constant [C<sub>3</sub>H<sub>6</sub>] and [2], the three ion-pairs appear to function under C–H conditions where the rate of ion-pair reorganization is faster than insertion (from both states). Clearly, the lack of information content inherent in the polymerization behavior of complex 2 is frustrating.

Fortunately, much less ambiguity exists with respect to the interpretation of the behavior of Hf complex 3 in the presence of various co-activators. On average, the PP tacticity decreases in the order B(C<sub>6</sub>F<sub>5</sub>)<sub>3</sub> > [Ph<sub>3</sub>C][B(C<sub>6</sub>F<sub>5</sub>)<sub>4</sub>] > PMAO, and, interestingly enough, only the latter two activators yield a catalyst that produces PP whose microstructure is sensitive to [C<sub>3</sub>H<sub>6</sub>] at 30 °C (Table 1). From the complete pentad distributions (see Table 2, entries 15, 19, and 23 and the Supporting Information), it is possible to model the observed behavior using two simple assumptions which will be discussed in order.

**Modeling of PP Microstructure Produced by Complex 3 – Scenario I –  $\alpha$ ,  $\beta$ , and *g/K* Are the Same.** The simplest explanation for the observed behavior is that, as with complex 2,  $\alpha$ ,  $\beta$ , and *g/K* are essentially unaffected by the nature of the counterion and that only  $\delta$  varies (Scenario I, parameters in Table 3). Figure 4a shows the fit of this model to the *mmmm* pentad of PP obtained under the different conditions in a plot of pentad intensity versus the variable  $\Delta$ ; given the experimental error inherent in the measurement of these stereosequence distributions as well as the reproducibility of polymerization experiments, it is clear that all of the data obtained using the different counterions and monomer concentrations can be adequately fit using this simple model.

**Scenario II –  $\alpha$ ,  $\beta$  Are the Same with *g/K* Different.** If one relaxes the restriction on *g/K*, allowing this parameter to “float” for the different cocatalysts (Scenario II), the overall fit

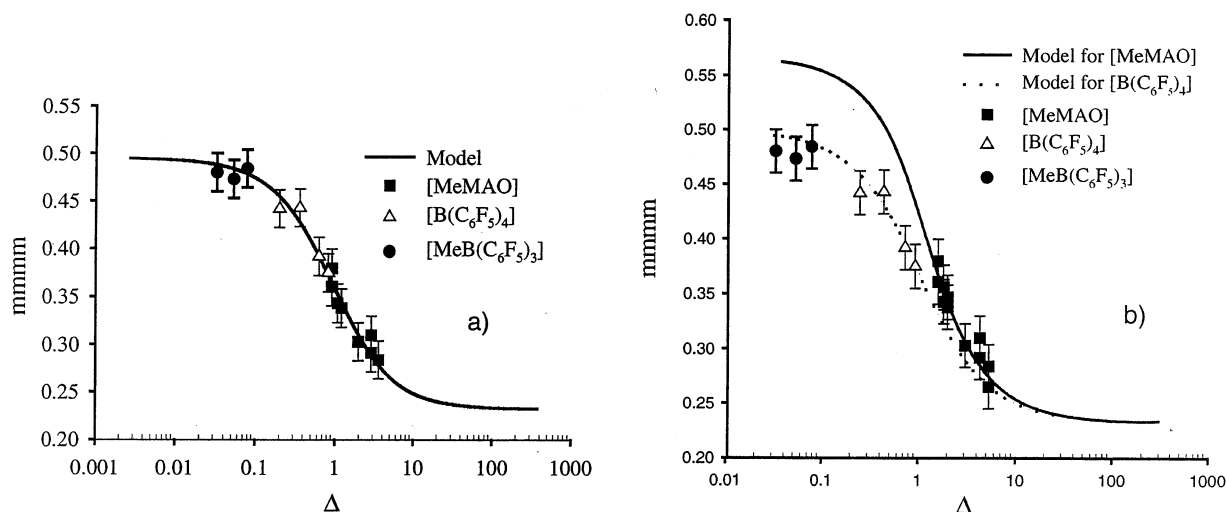


**Figure 4.**  $M^4$  pentad intensity vs  $\Delta$  for complex **3** activated by different cocatalysts: (a)  $\alpha$ ,  $\beta$ , and  $g/K$  are the same for all activators; (b)  $\alpha$  and  $\beta$  are the same but  $g/K$  is different for the three cocatalysts. Parameters and fits are summarized in Table 3, while representative experimental and calculated pentad distributions appear in Table 2.

of the model to all of the data is not noticeably improved despite the inclusion of an additional adjustable parameter (Table 3, Figure 4b). In particular, the modeling suggests that  $g/K$  is essentially identical for the  $B(C_6F_5)_3$ - and  $[Ph_3C][B(C_6F_5)_4]$ -activated catalyst while the PMAO-activated complex may have a higher value of  $g/K$ .

It should be mentioned that in earlier work<sup>9a</sup> significant correlation ( $-r^2 = 0.95$ ) existed between the estimated  $\alpha$  and  $g/K$  parameters for the PMAO-activated complex and so the current assumption of having all catalysts operating with the same values of  $\alpha$  and  $\beta$  (0.91 and 0.61, respectively) leads to a different estimate for  $g/K$  (i.e., 14 vs 9 in earlier work). In fact, this correlation is caused by the lack of asymptotic behavior observed for PP microstructure versus  $\Delta$  and thus ambiguous estimation of  $\alpha$  and  $\beta$  versus  $g/K$ .

In comparing the values of the parameters obtained for these two scenarios, as well as the goodness of the fit as reflected in the variance (Table 3), it is obvious that the principal effect on changing the counterion is one of changing the value of  $\delta$ , the ratio of the rate constants for insertion to inversion for the aspecific state (similar comments apply to the isospecific state as  $\delta \times g/K = k_p^\Delta/k_i$ ). In particular,  $\delta$  varies by more than an order of magnitude in going from  $B(C_6F_5)_3$  to PMAO with the  $[Ph_3C][B(C_6F_5)_4]$  intermediate between these two activators. In contrast, if  $g/K$  does vary (and this is by no means proven from the data), it does so by at most a factor of 3 for the different activators investigated.

As should be evident from the foregoing discussion, even with all of the available data, it was still necessary to make an assumption about this two-state catalyst, that  $\alpha$  and  $\beta$  (and likely  $g/K$ ) are the same for the different counterions, etc. While we have justified this assumption on the basis of literature precedent, intrinsically it is of interest to be able to address this issue — one needs a simpler system (i.e., one with fewer parameters) as in the following section.

**Modeling of PP Microstructure Produced by  $Me_2C(Cp)FluZrMe_2$  and Various Activators.** As mentioned in the Introduction, the activation of Ewen's prototypical  $C_s$ -symmetric metallocene complex  $Me_2C(Cp)FluZrMe_2$  using  $B(C_6F_5)_3$ ,  $[Ph_3C][B(C_6F_5)_4]$ , and  $[Ph_3C][FAl(o-C_6F_5-C_6F_4)_3]$  has been recently

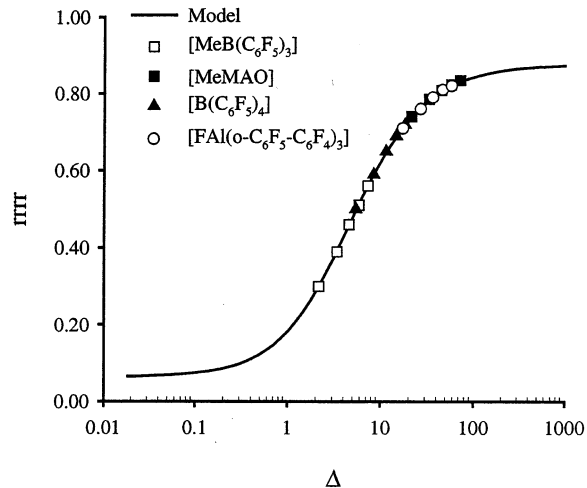


**Figure 5.**  $R^4$  pentad intensity vs  $\Delta$  for  $Me_2C(Cp)FluZrMe_2$  activated by  $B(C_6F_5)_3$ ,  $[Ph_3C][B(C_6F_5)_4]$ , PMAO, and  $[Ph_3C][FAl(o-C_6F_5-C_6F_4)_3]$  at 60 °C. Data are taken from ref 4b or are extrapolated from polymerization reactions conducted at 30–50 °C (ref 9a).

examined by Chen and Marks, and in particular the dependence of the pentad distribution on  $[C_3H_6]$  at 60 °C has been studied by these authors. Selected results, along with the calculated distributions obtained using our model, are summarized in Table 2, while a graphical representation of the  $rrrr$  pentad intensity versus  $\Delta$  appears in Figure 5.<sup>19</sup>

Here, there are only two parameters involved ( $\alpha$  and  $\delta$ ), and, at least at 60 °C, all of the data can be adequately fit by assuming that  $\alpha$  is the same for all counterions investigated (i.e.,  $\alpha \approx 0.974$ , Scenario I, Table 3) and that the only thing changing is the ratio of the rate constants for insertion to inversion (which in this case corresponds to  $\delta$  as both states are equivalent). In comparing  $B(C_6F_5)_3$  with  $[Ph_3C][B(C_6F_5)_4]$ , it is evident that a similar change in  $\delta$  is involved for this catalyst as compared to complex **3** and the change is in the same direction with the borane-activated complex functioning at lower values of  $\Delta = \delta[M]$ .

While we do not have access to strictly comparable data using PMAO as activator, it seems, on the basis of work performed

(19) We thank Prof. Marks for discussing these results prior to their publication.



**Table 4.** Temperature Dependence of  $\alpha$  and  $\delta$  Estimated from Modeling of Pentad Distributions<sup>a</sup>

$T$ (°C)	$[C_3H_6]$	MeB(C <sub>6</sub> F <sub>5</sub> ) <sub>3</sub>					B(C <sub>6</sub> F <sub>5</sub> ) <sub>4</sub>		FAl( <i>o</i> -C <sub>6</sub> F <sub>5</sub> -C <sub>6</sub> F <sub>4</sub> ) <sub>3</sub>				
		$\alpha$	$\delta$	$\sigma(\delta)^b$	$-r^2$	$\sigma^c$	$\alpha$	$\delta$	$\alpha$	$\delta$	$\sigma(\delta)^b$	$-r^2$	$\sigma^c$
-10	3.80	0.98 <sub>8</sub>	22.6	0.31	0.48	0.64	0.99 <sub>0</sub>	91.5	0.99 <sub>3</sub>				2.1
0	2.56	0.98 <sub>8</sub>	23.5	0.28	0.48	0.67	0.98 <sub>9</sub>	80.3	0.99 <sub>4</sub>				3.0
10	1.83	0.98 <sub>7</sub>	17.9	0.25	0.49	0.92	0.98 <sub>8</sub>	50.0	0.98 <sub>9</sub>	189	2.0	0.48	0.73
25	1.19	0.98 <sub>4</sub>	10.4	0.49	0.71	3.0	0.98 <sub>3</sub>	35.0	0.98 <sub>6</sub>	134	1.8	0.62	0.97
40	0.85	0.98 <sub>3</sub>	6.02	0.57	0.79	6.2	0.97 <sub>9</sub>	19.6	0.98 <sub>3</sub>	79.6	1.2	0.63	1.3
60	0.54	0.97 <sub>3</sub>	4.11	0.41	0.77	5.6	0.97 <sub>5</sub>	9.78	0.97 <sub>6</sub>	30.5	0.94	0.47	2.7

<sup>a</sup> Data from ref 4b. For calculated and observed pentad distributions, see Supporting Information. <sup>b</sup> Estimated standard deviation in the value of  $\delta$ . <sup>c</sup> Estimated standard deviation over all pentads ( $\times 10^2$ ).

earlier at 30–50 °C and the  $T$ -dependent behavior of PMAO-activated Me<sub>2</sub>C(Cp)IndZrCl<sub>2</sub>,<sup>9a</sup> that this catalyst resembles that activated by [Ph<sub>3</sub>C][FAl(*o*-C<sub>6</sub>F<sub>5</sub>-C<sub>6</sub>F<sub>4</sub>)<sub>3</sub>] – both function close to the KQ limit. It is perhaps appropriate to point out that the values of  $\delta$  obtained from modeling with these two activators (39.4 and 31.8, respectively, Table 3) correspond to  $\Delta\Delta G^\ddagger$  between inversion and insertion of 2.4<sub>3</sub> and 2.2<sub>9</sub> kcal mol<sup>-1</sup> at 60 °C. On this basis, it is perhaps correct to state that the differential effects of the counterion cannot be reliably interpreted in the case of these two activators, while, for example, the borane activated complex is significantly different!

In this simple, two parameter system, an examination of the error structure reveals no strong cross-correlation of  $\delta$  with  $\alpha$  when these are allowed to vary independently for the different counterions (data in Table 3, Scenario II). The same basic conclusion prevails, and only modest (and probably not significant given the errors involved) differences in  $\alpha$  between the different activators are noted. In essence, counterion effects manifest themselves mainly by altering the relative rates of insertion to inversion in C<sub>1</sub>- or C<sub>s</sub>-symmetric catalysts. Similarly, the modeling results with the C<sub>s</sub>-symmetric complex indicate that  $\alpha$  is largely unaffected by the nature of the counterion, and thus our earlier assumption seems quite reasonable in the context of an unsymmetrical system (3).

With these C<sub>s</sub>-symmetric complexes, as mentioned in the Introduction, it is possible to estimate both  $\alpha$  and  $\delta$  from single experiments. In the work of Chen and Marks, polymerization experiments were also performed at different  $T$  and at constant pressure (1 atm) with the different activators. The pentad distributions that result were analyzed using our model (see Supporting Information), and the parameters obtained are summarized in Table 4 along with estimates of errors in  $\delta$ , (negative) correlation coefficients between  $\alpha$  and  $\delta$ , and the overall fit of the model to the data.

As in earlier work,<sup>9a</sup> the  $T$  dependence of  $\alpha$  was flat over a small range, but in this case it is clear that, over a 70 °C range, these catalysts become more stereoselective at lower  $T$ . A more pronounced change in  $\delta$  is observed for all counterions over the same  $T$  range, and it is this feature which largely determines the appearance of the pentad distribution at any particular  $T$  with these catalysts.

It can be seen that the errors in  $\delta$  and the overall discrepancy between the model and the data are generally more significant under conditions that deviate most from KQ. This is easy to understand as the pentad distribution is a sensitive function of both  $\alpha$  and  $\delta$  under such conditions (i.e., eq 1), and more reliable parameter estimates are only available through study of this dependence through, for example, changes to  $[M]$ . This is evident in comparing the single point results obtained for the

borane-activated complex at 60 °C (Table 4) with those obtained from the experiments summarized in Table 3. Not only are the parameters somewhat different, but the fit of the model to the data is about 2.5 $\times$  worse for the single point experiment. Finally, as one approaches the KQ limit, it becomes impossible to reliably estimate  $\delta$  from a single point calculation; at the KQ limit, it is also impossible to estimate  $\delta$  even from experiments at different  $[M]$ . This is certainly true for the catalyst partnered with the fluoroaluminate counterion at low temperature where we were unable to provide meaningful estimates of  $\delta$  (Table 4).

This feature was also evident from plots of  $\ln(\delta)$  versus  $1/T$  where deviation from Arrhenius behavior was seen for some of the counterions at low  $T$ . This is a reflection of our inability to reliably estimate large values of  $\delta$  from single pentad distributions. From the slope of these plots,  $\Delta\Delta H^\ddagger$  for insertion versus inversion was estimated as -5.3, -6.2, and -8.2 kcal mol<sup>-1</sup> for the methylborate, borate, and aluminate counterions, while  $\Delta\Delta S^\ddagger = -13$ , -14, and -18 eu was similar for all three counterions. The values obtained for the fluoroaluminate counterion were based on the three highest  $T$ 's reported as significant downward curvature was observed in the Arrhenius plot at lower  $T$ .

## Conclusions

The polymerization experiments and modeling work presented here clearly indicate the origin of counterion effects on PP microstructure using two-state *ansa*-metallocene catalysts. In essence, of the fundamental parameters that are characteristic of these systems, it seems that  $\delta$  is the only one strongly affected by the counterion and that the ordering of the various counterions appears to be independent of catalyst structure/polymerization conditions at least for those systems functioning under intermediate conditions.

The only outstanding issue is whether  $g/K$  is affected by the nature of the counterion. Certainly our modeling of the data does not support a scenario where  $g/K$  must be different. It is plausible to argue that the most stable state in Scheme 1 is **B** (at least if X<sup>-</sup> is weakly coordinating) and thus  $K$ , as originally defined is  $>1$  and  $1/K < 1$ . Conversely, it is well known that, for many metallocene complexes, isospecific insertion is apparently faster than aspecific insertion and thus  $g$  is also expected to be  $>1$ . The net effect then is that  $g/K$  may not be a very sensitive indicator of counterion interactions as those factors which affect relative stability may have an opposite effect on reactivity.

In comparing complex **3** and Me<sub>2</sub>C(Cp)FluZrMe<sub>2</sub>, a more or less uniform ordering of the counterions can be discerned as far as their effect on  $\delta$  is concerned. However, it is evident that

the ordering of the counterion effect on  $\delta$  [i.e.,  $\text{MeB}(\text{C}_6\text{F}_5)_3 < \text{B}(\text{C}_6\text{F}_5)_4 < \text{FAl}(o\text{-C}_6\text{F}_5\text{-C}_6\text{F}_4)_3 \approx \text{PMAO}$ ] bears no strong resemblance to their coordinating ability [ $\text{FAl}(o\text{-C}_6\text{F}_5\text{-C}_6\text{F}_4)_3 \gg \text{MeB}(\text{C}_6\text{F}_5)_3 > \text{B}(\text{C}_6\text{F}_5)_4$ ] nor to trends in polymerization activity [ $\text{FAl}(o\text{-C}_6\text{F}_5\text{-C}_6\text{F}_4)_3 < \text{MeB}(\text{C}_6\text{F}_5)_3 \ll \text{B}(\text{C}_6\text{F}_5)_4$ ].

The observed behavior is counterintuitive; both inversion and insertion are either known<sup>1,20</sup> or thought<sup>21</sup> to involve the dissociation and/or displacement of the counterion. While there could easily be a differential effect on the rates of these two processes, thus leading to differences in  $\delta$ , one might expect the magnitude of this parameter to track with the coordinating ability of the counterion. However, it is possible that while intrinsic insertion rates are more sensitive to the nature of the counterion, inversion rates are less so. Thus, for example, the anomalous position of the  $\text{MeB}(\text{C}_6\text{F}_5)_3$  anion on the  $\Delta$  scale could simply reflect much lower insertion rates as compared to a lesser change in inversion rates.

At 25 °C where catalyst degradation is presumably less problematic, the activity data reported in ref 4b for the  $\text{B}(\text{C}_6\text{F}_5)_3$ ,  $[\text{Ph}_3\text{C}][\text{B}(\text{C}_6\text{F}_5)_4]$ , and  $[\text{Ph}_3\text{C}][\text{FAl}(o\text{-C}_6\text{F}_5\text{-C}_6\text{F}_4)_3]$ -activated  $\text{Me}_2\text{C}(\text{Cp})\text{FluZrMe}_2$  catalyst fall in the order  $A = 0.44, 8.9$ , and  $0.2 \times 10^6 \text{ g PP mol Zr}^{-1} \text{ atm}^{-1} \text{ h}^{-1}$ , respectively. Using our values of  $\delta$  determined for these counterions at 25 °C (Table 4), one can estimate that the relative rates of inversion are 28, 170, and 1, respectively, which is in qualitative agreement with the coordinating ability of these discrete counterions.<sup>22</sup>

We are, however, concerned whether the values obtained for  $\delta$  for the different counterions will quantitatively agree with measured inversion versus insertion rates. In particular, the rates of ion-pair reorganization of model ion-pairs **5** and **6** are some 300× faster for, for example,  $\text{B}(\text{C}_6\text{F}_5)_4$  versus  $\text{MeB}(\text{C}_6\text{F}_5)_3$  in  $\text{C}_6\text{D}_5\text{-Br}$  solution at the same  $[\text{Zr}]$  and  $T$  (see Supporting Information), yet  $\delta$  differs only by a factor of about 2 and in the wrong direction! Even more dramatic differences in inversion rates are reported for  $\text{MeB}(\text{C}_6\text{F}_5)_3^-$  versus  $\text{FAl}(o\text{-C}_6\text{F}_5\text{-C}_6\text{F}_4)_3^-$  partnered with  $\text{Me}_2\text{C}(\text{Cp})\text{FluZr}^+\text{Me}$  in toluene solution, and while the change is in the expected direction,  $\delta$  again only changes by about an order of magnitude as compared to a ca.  $10^3$  difference in inversion rates.<sup>4</sup>

We suspect the discrepancy here may reflect the choice of model ion-pair (or medium) used to determine inversion rates. Beswick and Marks have recently noted pronounced steric effects on the rate of ion-pair reorganization in  $[(1,2\text{-Me}_2\text{-Cp})_2\text{ZrR}][\text{MeB}(\text{C}_6\text{F}_5)_3]$  ion-pairs with sterically hindered  $\text{Zr-R}$  groups exhibiting lower barriers to reorganization.<sup>23</sup> Differences in free energies of activation as large as  $\sim 4 \text{ kcal mol}^{-1}$  for  $\text{Zr-Me}$  versus  $\text{Zr-CH}_2\text{tBu}$  have been reported. The latter value corresponds to a rate difference of 850 at 25 °C and provides a reasonable explanation of why the  $\text{B}(\text{C}_6\text{F}_5)_3$ -activated complexes appear to operate at significantly lower values of  $\Delta$ ; in essence, these catalysts have both (moderately) slower insertion rates coupled with a dramatic increase in ion-pair reorganization rates following initiation. The latter hypothesis is also consistent

with recent work from the Landis group on low  $T$  detection of propagating ion-pairs where the  $\text{MeB}(\text{C}_6\text{F}_5)_3$  counterion appears to be less coordinating during 1-hexene polymerization.<sup>20</sup>

Finally, why do some catalysts when activated with the same cocatalyst appear to operate under C-H conditions (e.g., **2** or **4**), while others have intermediate behavior (e.g., **3**) or exhibit highly alternating insertion [e.g.,  $\text{Me}_2\text{C}(\text{Cp})\text{FluZrMe}_2$ ], despite similar polymerization rates? For example, in the case of the PMAO-activated hafnocenes **3** and **4**, the latter is about 4× more active than the former under the same conditions (Table 1), and yet **3** functions under intermediate conditions ( $\Delta \approx 1$ ), while **4** behaves like a single-state catalyst ( $\Delta < 0.1$ ).

This result implies that the rate of ion-pair reorganization differs greatly with the Si-bridged complex undergoing this process 1–2 orders of magnitude faster than the C-bridged catalyst! As alluded to earlier, the rates of ion-pair reorganization are different for ion-pairs derived from Zr complexes **2** or **1** and  $\text{B}(\text{C}_6\text{F}_5)_3$  with the Si-bridged complex showing a significantly higher rate (ca. 30× higher) based on EXSY spectra at different mixing times. This result is consistent with the observed behavior of their Hf analogues in propylene polymerization. Experiments underway will clarify whether the observed differences in rate are large enough to counterbalance the modest activity difference between these two systems.

## Experimental Section

**General.** All solvents and chemicals were reagent grade and purified as required. All synthetic reactions were conducted under an atmosphere of dry nitrogen in dry glassware unless otherwise noted. Tetrahydrofuran, diethyl ether, hexane, toluene, and dichloromethane were dried and deoxygenated by passage through columns of A2 alumina and Q5 deoxo catalyst as described in the literature.<sup>24</sup>

The ligands  $\text{Me}_2\text{C}(\text{IndH})\text{CpH}$  and  $\text{Me}_2\text{Si}(\text{IndH})\text{CpH}$  were prepared according to reported procedures.<sup>8i,25</sup> The compounds  $\text{Zr}(\text{NMe}_2)_4$  and  $\text{Hf}(\text{NMe}_2)_4$  were prepared as described in the literature.<sup>26</sup> Amine elimination reactions<sup>26</sup> were used to prepare the  $\text{Me}_2\text{X}(\text{Ind})\text{CpM}(\text{NMe}_2)_2$  complexes following published procedures ( $\text{X} = \text{C}, \text{M} = \text{Zr}, \text{Hf}, \text{X} = \text{Si}, \text{M} = \text{Zr}$ )<sup>8i,27</sup> or as described elsewhere ( $\text{X} = \text{Si}, \text{M} = \text{Hf}$ ).<sup>28</sup> These compounds could be converted to the known dichloride complexes<sup>8i,25,27</sup> by reaction with excess  $\text{Me}_3\text{SiCl}$ .<sup>26</sup> The zirconium dimethyl complexes **1** and **2** could be prepared by alkylation of the latter compounds with MeLi as described below. For the hafnium dimethyl complexes **3** and **4**, the procedure of Kim and Jordan<sup>26e</sup> was employed using the bis-(dimethylamido) complexes and  $\text{AlMe}_3$  as described below.  $\text{MeAl}(\text{BHT})_2$  was prepared using the method reported by Ittel and co-workers<sup>29</sup> and was added to toluene solvent (ca. 50–100  $\mu\text{M}$ ) used to dilute stock solutions of compounds **1–4** or cocatalysts prior to delivery to the reactor. The activators  $\text{B}(\text{C}_6\text{F}_5)_3$  and  $[\text{Ph}_3\text{C}][\text{B}(\text{C}_6\text{F}_5)_4]$  were generously donated by Nova Chemicals Ltd.

- (20) For relevant experimental work on borane-activated catalysts, see: Landis, C. R.; Rosaeen, K. A.; Sillars, D. R. *J. Am. Chem. Soc.* **2003**, *125*, 1710–1711.
- (21) For theoretical work on the involvement of the counterion on insertion, see: (a) Lanza, G.; Fraga, I. L.; Marks, T. J. *J. Am. Chem. Soc.* **2000**, *122*, 12764–12777. (b) Chan, M. S. W.; Ziegler, T. *Organometallics* **2000**, *19*, 5182–5189. (c) Vanka, K.; Ziegler, T. *Organometallics* **2001**, *20*, 905–913.
- (22) We thank a reviewer for suggesting this type of analysis.
- (23) Beswick, C. L.; Marks, T. J. *J. Am. Chem. Soc.* **2000**, *122*, 10358–10370.

- (24) Pangborn, A. B.; Giardello, M. A.; Grubbs, R. H.; Rosen, R. K.; Timmers, F. J. *Organometallics* **1996**, *15*, 1518–1520.
- (25) Green, M. L. H.; Ishihara, N. J. *Chem. Soc., Dalton Trans.* **1994**, 657.
- (26) (a) Hughes, A. K.; Meetsma, A.; Teuben, J. H. *Organometallics* **1993**, *12*, 1936. (b) Herrmann, W. A.; Morawietz, M. J. A. *J. Organomet. Chem.* **1994**, *482*, 169. (c) Diamond, G. M.; Rodewald, S.; Jordan, R. F. *Organometallics* **1995**, *14*, 5. (d) Carpenetti, D. W.; Kloppenberg, L.; Kupec, J. T.; Peterson, J. L. *Organometallics* **1996**, *15*, 1572. (e) Kim, I.; Jordan, R. F. *Macromolecules* **1996**, *29*, 489. (f) Diamond, G. M.; Jordan, R. F.; Petersen, J. L. *J. Am. Chem. Soc.* **1996**, *118*, 8024. (g) Diamond, G. M.; Jordan, R. F.; Petersen, J. L. *Organometallics* **1996**, *15*, 4530. (h) Diamond, G. M.; Jordan, R. F.; Petersen, J. L. *Organometallics* **1996**, *15*, 4038.
- (27) Herrmann, W. A.; Morawietz, M. J. A.; Priemeier, T. J. *Organomet. Chem.* **1996**, *506*, 351.
- (28) Mohammed, M. Ph.D. Thesis, University of Waterloo, 2001.
- (29) Shreve, A. P.; Mulhaupt, R.; Fultz, W.; Calabrese, J.; Robbins, W.; Ittel, S. D. *Organometallics* **1988**, *7*, 409–416.

Routine  $^1\text{H}$  and  $^{13}\text{C}$  NMR spectra were recorded in benzene- $d_6$  or  $\text{CDCl}_3$  solution on either a Bruker AM-250, AC-200, or AC-300 spectrometer.  $^1\text{H}$  and  $^{19}\text{F}$  NMR spectra of ion-pairs were recorded using an AC-200 or Varian Mercury 300 or Innova 400 spectrometer in toluene- $d_8$  or bromobenzene- $d_5$  solution with 2,3,5,6-tetrafluoro-*p*-xylene as an internal standard. Elemental analyses were determined by Oneida Research Services, Inc., New York.

**Polymerization Procedures and Polymer Characterization.** Propylene polymerization in toluene solvent and characterization of poly(propylene) involved techniques and methods that have been presented in detail elsewhere.<sup>8f</sup> Propylene solubility in toluene as a function of *P,T* was estimated from literature data,<sup>30</sup> and these concentrations appear in Table 1. Mass transfer limitations can significantly affect PP MWD and microstructure even using single-site catalysts if the polymer formed is soluble in the reaction medium;<sup>9</sup> diffusion-limited, polymerization experiments in toluene can be detected by variation in monomer flow with, for example, stirring speed. All polymerization experiments reported here were conducted at catalyst concentrations and at stirring speeds (1000 rpm) such that intrinsic behavior was studied. Temperature control was generally better than  $\pm 1^\circ\text{C}$  following catalyst introduction, and catalyst concentrations were chosen so as to avoid exothermic conditions.

Polymerization reactions were typically conducted for periods of time corresponding to attainment of steady state as revealed by a stable mass flow profile (see Figure 2) and then for an additional period equal to the length of time required to reach steady state in most cases. Reactions were halted by venting the monomer and emptying the reactor contents into a round-bottomed flask containing methanol. Solvent was partially evaporated to dryness in vacuo, and then the syrup was transferred to an aluminum pie plate. Solvent was allowed to further evaporate at room temperature in a hood and then at  $60^\circ\text{C}$  in a vacuum oven ( $\sim 1\text{ mmHg}$ ).

Samples for GPC analysis were obtained by Soxhlet extraction of a portion of the polymer with refluxing toluene containing 0.1 wt % Irganox 1010 as an antioxidant. The soluble extracts were concentrated to dryness under high vacuum, and the purified polymer was dissolved in TCB (ca. 0.1–0.5 wt %) containing 0.1 wt % Irganox. The solutions were then analyzed after dissolution periods of 1–3 h at  $150^\circ\text{C}$  using a Waters 150C+ instrument as described elsewhere.<sup>8f</sup> It is important to use antioxidant during Soxhlet extraction and to minimize dissolution time at  $150^\circ\text{C}$  to prevent thermal degradation of the polymer.

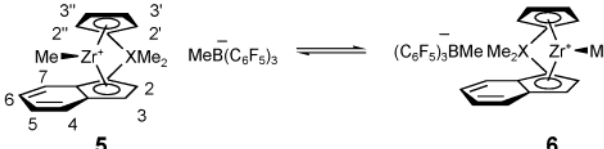
**Propylene Polymerization Using Borane or Borate Activators.** An autoclave reactor containing 480 mL of toluene and 1.0 g (ca. 2 mmol) of MAD was saturated with propylene at  $30^\circ\text{C}$  at the desired pressure for several hours until monomer flow had effectively ceased. After another hour, solutions of the ion-pairs or dialkyl and cocatalyst were added in the same manner as described below.

In the case of  $\text{B}(\text{C}_6\text{F}_5)_3$ , a solution of the ion-pairs [7.5 mM in complexes 1–3 and 9 mM in  $\text{B}(\text{C}_6\text{F}_5)_3$  B:M = 1.2:1] was prepared by mixing stock solutions of each component at room temperature. One milliliter of this solution was transferred into a 50 mL sample bomb and diluted with 19.0 mL of toluene prepurified using MAD. After a period of 5–10 min, the contents were delivered to the reactor using a 10 psi overpressure of dry  $\text{N}_2$ .

In the case of  $[\text{Ph}_3\text{C}][\text{B}(\text{C}_6\text{F}_5)_4]$ , a similar procedure was employed except 10.0 mL of a solution of  $[\text{Ph}_3\text{C}][\text{B}(\text{C}_6\text{F}_5)_4]$  (0.15–0.30 mM depending on metal and  $[\text{C}_3\text{H}_6]$ ) was added to the reactor followed by 10.0 mL of a solution of 1–3 (0.125–0.25 mM B:M = 1.2:1) within a minute or less.

**Preparation of  $\text{Me}_2\text{C}(\text{Ind})\text{CpZrMe}_2$  (1).** A suspension of  $\text{Me}_2\text{C}(\text{Ind})\text{CpZrCl}_2$  (191 mg, 0.5 mmol) in 25 mL of diethyl ether was cooled to  $-78^\circ\text{C}$ , and MeLi (1.0 mL of 1.0 M solution in ether, 1.0 mmol) was added via a syringe while stirring. The solution was allowed to

**Table 5.**  $^1\text{H}$  NMR Shift Data for Ion-Pairs Formed from Complexes 1,2 and  $\text{B}(\text{C}_6\text{F}_5)_3$ <sup>a</sup>



assignment	X = C (4:1)		X = Si (3:1)	
	major (5)	minor (6)	major (5)	minor (6)
H <sub>4</sub>	7.13 (d)		7.23 (d)	7.13
H <sub>5</sub>	6.88 (t)		7.00 (t)	6.41
H <sub>6</sub>	6.52 (t)		6.65 (t)	
H <sub>7</sub>	6.67 (d)		6.59 (d)	6.84
H <sub>3</sub>	6.25 (d)	6.35 (d)	6.54 (d)	6.70 (d)
H <sub>3''</sub>	5.95 (dd)	5.66 (dd)	6.25 (dd)	5.87 (dd)
H <sub>3'</sub>	5.86 (dd)	6.06 (dd)	6.07 (dd)	6.38 (dd)
H <sub>2</sub>	5.49 (d)	4.72 (d)	5.65 (d)	5.07 (d)
H <sub>2'</sub>	5.06 (dd)	5.25 (dd)	5.32 (dd)	4.85 (dd)
H <sub>2''</sub>	4.40 (dd)	4.39 (dd)	4.85 (dd)	5.37 (dd)
XMe <sub>2</sub>	1.21 (s)	1.27 (s)	0.17 (s)	0.28 (s)
XMe <sub>2</sub>	1.10 (s)	0.88 (s)	0.11 (s)	−0.01 (s)
BMe	0.81 (br s)	−0.26 (br s)	0.53 (br s)	−0.54 (br s)
ZrMe	−0.85 (s)	0.44 (s)	−0.84 (s)	0.54 (s)

<sup>a</sup> Toluene- $d_8$  solution, 298 K, 300 MHz. Assignments based on NOESY and COSY spectra.

warm slowly to room temperature, and stirring was continued for an additional 1 h after reaching room temperature. The reaction mixture was filtered via a cannula, and the ether was removed in vacuo. The off-white solid was dissolved in a minimum amount of pentane and was cooled to  $-35^\circ\text{C}$  overnight. The supernatant was decanted, and the crystals were washed with cold pentane. The crystalline material was dried under vacuum in a glovebox to give 113 mg (66% yield) of spectroscopically pure compound 1.  $^1\text{H}$  NMR (250 MHz,  $\text{C}_6\text{D}_6$ ):  $\delta$  7.46 (d,  $J = 8.6\text{ Hz}$ , 1H, H<sub>4</sub>), 7.23 (d,  $J = 8.9\text{ Hz}$ , 1H, H<sub>7</sub>), 7.10 (m, 1H, H<sub>5</sub>), 6.78 (m, 1H, H<sub>6</sub>), 6.64 (d,  $J = 3.4\text{ Hz}$ , 1H, H<sub>3</sub>), 6.30 (m, 1H, H<sub>3'</sub>), 6.25 (m, 1H, H<sub>3''</sub>), 5.52 (d,  $J = 3.5\text{ Hz}$ , 1H, H<sub>2</sub>), 5.30 (dd,  $J = 2.5\text{ Hz}$ , 1H, H<sub>2'</sub>), 5.14 (dd,  $J = 2.5\text{ Hz}$ , 1H, H<sub>2''</sub>), 1.51 (s, 3H, Me<sub>2</sub>C), 1.32 (s, 3H, Me<sub>2</sub>C), 0.06 (s, 3H, Me–Zr), −1.01 (s, 3H, Me–Zr).  $^{13}\text{C}$  NMR (50.32 MHz,  $\text{C}_6\text{D}_6$ ):  $\delta$  125.9, 124.1, 123.8, 123.7, 119.3, 114.7, 113.8, 113.4, 113.0, 104.6, 103.9, 103.3, 38.4, 34.5, 30.7, 26.3, 25.4. Anal. Calcd for  $\text{C}_{19}\text{H}_{22}\text{Zr}$ : C, 66.81; H, 6.49. Found: C, 66.59; H, 6.39.

**Preparation of  $\text{Me}_2\text{Si}(\text{Ind})\text{CpZrMe}_2$  (2).** A suspension of  $\text{Me}_2\text{Si}(\text{Ind})\text{CpZrCl}_2$  (199 mg, 0.5 mmol) in 25 mL of diethyl ether was cooled to  $-78^\circ\text{C}$ , and MeLi (1.0 mL of 1.0 M solution in ether, 1.0 mmol) was added via a syringe into the suspension while stirring. The solution was allowed to warm to  $0^\circ\text{C}$  and was stirred at this temperature for an additional 1.5 h. The reaction mixture was filtered to remove LiCl, and the ether was removed in vacuo. The off-white residue was dissolved in a minimum amount of pentane and was cooled to  $-35^\circ\text{C}$  overnight. The supernatant was decanted, and the crystals were washed with cold pentane. The crystalline material was dried under vacuum in a glovebox to give 122 mg (68% yield) of spectroscopically pure compound 2.  $^1\text{H}$  NMR (250 MHz,  $\text{C}_6\text{D}_6$ ):  $\delta$  7.63 (br d,  $J = 8.6\text{ Hz}$ , 1H, H<sub>7</sub>), 7.20 (m, 2H, H<sub>4</sub>–H<sub>5</sub>), 6.89 (d,  $J = 3.3\text{ Hz}$ , 1H, H<sub>6</sub>), 6.63 (m, 1H, H<sub>3</sub>), 6.60 (dd,  $J = 2.9\text{ Hz}$ , 1H, H<sub>3'</sub>), 6.53 (dd,  $J = 2.9\text{ Hz}$ , 1H, H<sub>3''</sub>), 5.70 (d,  $J = 3.3\text{ Hz}$ , 1H, H<sub>2</sub>), 5.48 (dd,  $J = 2.9\text{ Hz}$ , 1H, H<sub>2'</sub>), 5.37 (dd,  $J = 2.9\text{ Hz}$ , 1H, H<sub>2''</sub>), 0.44 (s, 3H, Me<sub>2</sub>Si), 0.31 (s, 3H, Me<sub>2</sub>Si), 0.12 (s, 3H, Me–Zr), −1.90 (s, 3H, Me–Zr).  $^{13}\text{C}$  NMR (50 MHz,  $\text{C}_6\text{D}_6$ ):  $\delta$  130, 126.9, 125.9, 125.0, 124.5, 120.6, 119.3, 118.5, 112.8, 112.2, 114.4, 35.2, 31.1, −3.2, −4.2. Anal. Calcd for  $\text{C}_{18}\text{H}_{22}\text{SiZr}$ : C, 60.44; H, 6.20. Found: C, 60.50; H, 6.35.

**Preparation of  $\text{Me}_2\text{C}(\text{Ind})\text{CpHfMe}_2$  (3).** A suspension of  $\text{Me}_2\text{C}(\text{Ind})\text{CpHf}(\text{NMe}_2)_2$  (2.44 g, 5.0 mmol) in 25 mL of hexane was cooled to  $-35^\circ\text{C}$ , and neat trimethylaluminum (1.44 g, 20 mmol) at  $-35^\circ\text{C}$

(30) (a) Atiqullah, M.; Hammawa, H.; Hamid, H. *Eur. Polym. J.* **1998**, *34*, 1511–1520. (b) Reid, R. R.; Prausnitz, J. M.; Poling, B. E. *The Properties of Gases & Liquids*; McGraw-Hill: Singapore, 1987.

was added into the suspension while stirring. The solution was warmed to ambient temperature and stirred overnight. The reaction mixture was vacuum-dried to provide crude product, which was recrystallized in hexane at  $-35\text{ }^{\circ}\text{C}$  to provide spectroscopically pure **3** as an off-white, crystalline powder in 96% yield.  $^1\text{H}$  NMR (300 MHz,  $\text{C}_6\text{D}_6$ ):  $\delta$  7.42 (d,  $J = 8.6\text{ Hz}$ , 1H, H7), 7.23 (dd,  $J = 8.7, 1.0\text{ Hz}$ , 1H, H4), 7.05 (dd,  $J = 8.6, 7.0\text{ Hz}$ , 1H, H5), 6.74 (dd,  $J = 8.6, 7.0\text{ Hz}$ , 1H, H6), 6.52 (d,  $J = 3.3\text{ Hz}$ , 1H, H3), 6.18 (dd,  $J = 3.2, 2.4\text{ Hz}$ , 1H, H3'), 6.11 (dd,  $J = 3.2, 2.4\text{ Hz}$ , 1H, H3''), 5.40 (d,  $J = 3.3\text{ Hz}$ , 1H, H2), 5.16 (dd,  $J = 3.2, 2.4\text{ Hz}$ , 1H, H2'), 5.03 (dd,  $J = 3.2, 2.4\text{ Hz}$ , 1H, H2''), 1.55 (s, 3H,  $\text{Me}_2\text{C}$ ), 1.33 (s, 3H,  $\text{Me}_2\text{C}$ ),  $-0.12$  (s, 3H, Me–Hf),  $-1.20$  (s, 3H, Me–Hf).  $^{13}\text{C}$  NMR (75 MHz,  $\text{C}_6\text{D}_6$ ):  $\delta$  126.5, 126.0, 124.3, 123.9, 123.7, 118.8, 116.6, 114.1, 113.0, 112.3, 103.3, 103.2, 102.7, 39.3, 38.4, 37.9, 26.4, 25.4.

**Preparation of  $\text{Me}_2\text{Si}(\text{Ind})\text{CpHfMe}_2$  (**4**).** A suspension of  $\text{Me}_2\text{Si}(\text{Ind})\text{CpHf}(\text{NMe}_2)_2$  (1.206 g, 2.4 mmol) in 20 mL of hexane was cooled to  $-35\text{ }^{\circ}\text{C}$ , and neat  $\text{AlMe}_3$  (0.69 g, 9.6 mmol) at  $-35\text{ }^{\circ}\text{C}$  was added to the suspension while stirring. The solution was warmed to ambient temperature and stirred overnight. The reaction mixture was dried to provide crude product, which was recrystallized in hexane at  $-35\text{ }^{\circ}\text{C}$  to provide spectroscopically pure **4** as an off-white, crystalline powder in >95% yield.  $^1\text{H}$  NMR (300 MHz,  $\text{C}_6\text{D}_6$ ):  $\delta$  7.55 (d,  $J = 8.6\text{ Hz}$ , 1H, H7), 7.16 (m, 1H, H4), 7.12 (m, 1H, H5), 6.86 (m, 1H, H6), 6.82 (dd,  $J = 3.0\text{ Hz}$ , 1H, H3), 6.47 (dd,  $J = 1.7\text{ Hz}$ , 1H, H3'), 6.39 (dd,  $J = 1.9\text{ Hz}$ , 1H, H3''), 5.59 (dd,  $J = 3.0\text{ Hz}$ , 1H, H2), 5.37 (dd,  $J = 2.4\text{ Hz}$ , 1H, H2'), 5.30 (dd,  $J = 2.4\text{ Hz}$ , 1H, H2''), 0.41 (s, 3H,  $\text{Me}_2\text{Si}$ ),

0.29 (s, 3H,  $\text{Me}_2\text{Si}$ ),  $-0.16$  (s, 3H, Me–Hf),  $-1.28$  (s, 3H, Me–Hf).  $^{13}\text{C}$  NMR (75 MHz,  $\text{C}_6\text{D}_6$ ):  $\delta$  130.0, 126.6, 125.9, 125.2, 125.0, 124.7, 120.1, 118.7, 117.6, 111.7, 111.5, 110.5, 40.1, 38.0,  $-3.3$ ,  $-4.1$ .

**Formation of Ion-Pairs **5** and **6** from Complexes **1,2** and **B**( $\text{C}_6\text{F}_5$ )<sub>3</sub> in Toluene- $d_8$ .** Stock solutions of  $\text{Me}_2\text{X}(\text{Ind})\text{CpZrMe}_2$  (**1**) (0.05 M) and  $\text{B}(\text{C}_6\text{F}_5)_3$  (0.050 M) in toluene- $d_8$  were mixed in a 1:1 ratio at  $-35\text{ }^{\circ}\text{C}$  in a glovebox. The immediate color change from colorless to orange red, upon mixing the two stock solutions, indicated a rapid reaction at this temperature. The  $^1\text{H}$  and  $^{19}\text{F}$  NMR spectra of the resulting solution show two sets of signals in a roughly 1:3 ( $\text{X} = \text{Si}$ ) or 1:4 ( $\text{X} = \text{C}$ ) ratio at ambient temperature. The  $^1\text{H}$  NMR chemical shifts of the ion-pairs formed are listed in Table 5.

**Acknowledgment.** The authors would like to thank the Natural Sciences and Engineering Research Council and Nova Chemicals Ltd. of Canada, and the University of Akron for financial support of this work. M.N. wishes to thank CNPq (Conseil Nacional de Pesquisa – Brazil) under the program PROFIX for providing a scholarship.

**Supporting Information Available:** Observed and calculated pentad distributions and 1D and 2D NMR spectra of ion-pairs **5** and **6** (PDF). This material is available free of charge via the Internet at <http://pubs.acs.org>.

JA0207706